

# Spiral regularities in magnetic field variations and auroras

Y. I. Feldstein<sup>1</sup>, L. I. Gromova<sup>1</sup>, M. Förster<sup>2</sup>, and A. E. Levitin<sup>1</sup>

<sup>1</sup>Institute of Terrestrial Magnetism, Ionosphere, and Radiowave Propagation of the Russian Academy of Sciences (IZMIRAN), 142090 Troitsk, Moscow region, Russia

<sup>2</sup>Helmholtz-Zentrum Potsdam, GFZ German Research Centre for Geosciences, 14473 Potsdam, Germany

**Abstract.** The conception of spiral shaped precipitation regions, where solar corpuscles penetrate the upper atmosphere, was introduced into geophysics by C. Størmer and K. Birkeland at the beginning of the last century. Later, in the course of the XX-th century, spiral distributions were disclosed and studied in various geophysical phenomena. Most attention was devoted to spiral shapes in the analysis of regularities pertaining to the geomagnetic activity and auroras.

We review the historical succession of perceptions about the number and positions of spiral shapes, that characterize the spatial-temporal distribution of magnetic disturbances. We describe the processes in the upper atmosphere, which are responsible for the appearance of spiral patterns. We considered the zones of maximal aurora frequency and of maximal particle precipitation intensity, as offered in the literature, in their connection with the spirals.

We discuss the current system model, that is closely related to the spirals and that appears to be the source for geomagnetic field variations during magnetospheric substorms and storms. The currents in ionosphere and magnetosphere constitute together with field-aligned (along the geomagnetic field lines) currents (FACs) a common 3-D current system. At ionospheric heights, the westward and eastward electrojets represent characteristic elements of the current system. The westward electrojet covers the longitudinal range from the morning to the evening hours, while the eastward electrojet ranges from afternoon to near-midnight hours. The polar electrojet is positioned in the dayside sector at cusp latitudes. All these electrojets map along the magnetic field lines to certain plasma structures in the near-Earth space. The first spiral distribution of auroras was found based on observations in Antarctica for the nighttime-evening sector (N-spiral), and later in the nighttime-evening (N-spiral) and morning (M-spiral) sectors both in the Northern and Southern Hemispheres. The N and M spirals drawn in polar coordinates form an oval, along which one observes most often auroras in the zenith together with a westward electrojet.

The nature of spiral distributions in geomagnetic field variations was unambiguously interpreted after the discovery of the spiral's existence in the auroras had been established and this caused a change from the paradigm of the auroral zone to the paradigm of the auroral oval. Zenith forms of auroras are found within the boundaries of the auroral oval. The oval is therefore the region of most frequent precipitations of corpuscular fluxes with auroral energy, where anomalous geophysical phenomena occur most often and with maximum intensity.

S. Chapman and L. Harang identified the existence of a discontinuity at auroral zone latitudes ( $\Phi \sim 67^\circ$ ) around midnight between the westward and eastward electrojets, that is now known as the Harang discontinuity. After the discovery of the auroral oval and the position of the westward electrojet along the oval, it turned out, that there is no discontinuity at a fixed latitude between the opposite electrojets, but rather a gap, the latitude of which varies smoothly between  $\Phi \sim 67^\circ$  at midnight and  $\Phi \sim 73^\circ$  at 20 MLT. In this respect the term "Harang discontinuity" represents no intrinsic phenomenon, because the westward electrojet does not experience any disruption in the midnight sector but continues without breaks from dawn to dusk hours.

**Keywords.** spirals, auroral oval, auroral forms, high-latitude magnetic variations, field-aligned currents, equivalent ionospheric currents, dynamo theory

## 1 Introduction

1.1. This review is dedicated to one of the branches of planetary-scale research on geomagnetic field variations and the morphology of discrete auroral forms – the spiral distributions, which are used in geophysics for the description of various phenomena. A comprehensive view of the results obtained in the scientific literature is given, in particular the contributions in Russian language. Such information will be most notably interesting and useful for those scientists, who often have problems to get proper access to scientific publications in Russian tongue either due to the language barrier or because of undue hardship to obtain such informations, which are buried in Institute’s collections or in particular topical proceedings. The scientific development in the USSR, including geophysics, was detached to a large extent from global science progress for a long time period. Only the participation of the Soviet Union in the International Geophysical Year (1957-1958) and in subsequent international geophysical projects changed the situation fundamentally. There arose the additional possibility for publications in international journals, but many results continued to be known primarily in Russia only and were not cited in the global literature. We hope that the present review attracts attention to researchers in the field of Earth’s magnetism and auroras, as they are such phenomena that intrigues mankind’s exploratory spirit for many centuries. The following elaborations about the development of scientific knowledge on a specific geophysical problem might also be interesting for historians of science.

1.2. The conception of spirals, along which the precipitation of corpuscular solar fluxes occur, is closely related to the model experiments of Kristian Birkeland (Birkeland, 1908, 1913) and the theoretical calculations of Carl Størmer (Størmer, 1917a,b, 1955). Birkeland illuminated a magnetised model sphere (“terrella”) representing the Earth by bundles of low-energy electrons. The bundles of charged particles were bent towards the night side of the terrella and toward the magnetic poles. The regions of precipitation were made visible through a phosphorescent layer which covered the terrella. Glowing stripes, one in each hemisphere, surrounded in the experiments the magnetic poles of the terrella. The stripe winded up around the near-pole region of the Northern Hemisphere in counter-clockwise direction. The terrella experiments have been repeated and extended by Bruce (1931).

1.3 Størmer (1917a,b, 1955) developed the methodology and performed mathematical calculations of the trajectories of positively charged particles (protons and  $\alpha$ -particles) and of electrons in a dipole magnetic field. Figure 1 shows results of Størmer’s calculations for the distribution of precipitations of positively charged particles at high latitudes of the

Northern Hemisphere. The entire precipitation region has been obtained by a series of calculated orbits. It explains the formation of a spiral shaped region of precipitation in Birkeland’s terrella experiment. This “laboratory” spiral has been obtained from calculations, adopting particular values of the  $\gamma$ -parameter (constant of integration) and of  $\Psi$  (declination of the corpuscles’ source region). In the theory of Størmer,  $\gamma$  can assume arbitrary values, while the sun’s declination  $\Psi$  varies in the course of the year by  $\pm 34^\circ$  with respect to the equatorial plane of the dipole. The “laboratory” spiral in Fig. 1 results from a  $\sim 1$ -year long integration time of the calculations. Not the whole spiral in Fig. 1 corresponds to a given UT moment with its particular  $\Psi$  value, but only a few discrete points along the spiral.

1.4 The variation of  $\Psi$  along the spiral is non-uniform; there is rather a bunching of points within four sectors, centred around  $\Psi = 0$ , i.e., close to the equinoctial periods. The higher density of points occurs near 03, 09, 14, and 20 hours local time, when the direction of the corpuscular source region varies most quickly.

1.5 In order to move the theoretical auroral spiral to the  $\sim 23^\circ$  colatitude required for agreement with auroral observations during the night time, Størmer postulated the existence of a ring current at higher geocentric distances. The magnetic field of this current deflects the path of solar particles, so that they precipitate at lower latitudes, but at the Earth’s surface its field strength is small.

1.6 Precipitations of charged particles into the upper atmosphere leads to a series of phenomena. Certainly it could be assumed that the most intense specific geophysical phenomena, caused by these precipitations, occur along the spirals, which are oriented in a determinate way according to the sun’s direction. The precipitation region in the upper atmosphere has the form of a spiral in the coordinates of magnetic latitude versus magnetic local time. At the Northern Hemisphere, the spiral wind up clockwise from the magnetic pole for positively charged particles and in anti-clockwise directions for electrons.

1.7 Based on observations of the geomagnetic field, Birkeland (1908, 1913) concluded that the magnetic disturbances and the closely related aurorae are caused by the precipitation of electrically charged particles from the sun into the upper atmospheric layers. He assumed that the currents, calculated from the geomagnetic perturbations are real free currents, probably consisting of free electrons coming in from space towards the auroral zone and bent back again. The problem of the Birkeland–Størmer theory consisted in the unsteadiness of solar charged particle fluxes of one polarity, which are dissipated before they can reach the Earth. The energy of protons with a flux velocity of  $\sim 500$  km/s amount to a few keV. Such a particle velocity within the flux was deduced from the time lag of the beginning of magnetic disturbances on Earth with respect to the flare at the sun. This lag comes along with the ejection of a particle flux, the subsequent development of a magnetic storm and the appearance of auro-

Correspondence to: Y. I. Feldstein  
afeld@aol.com

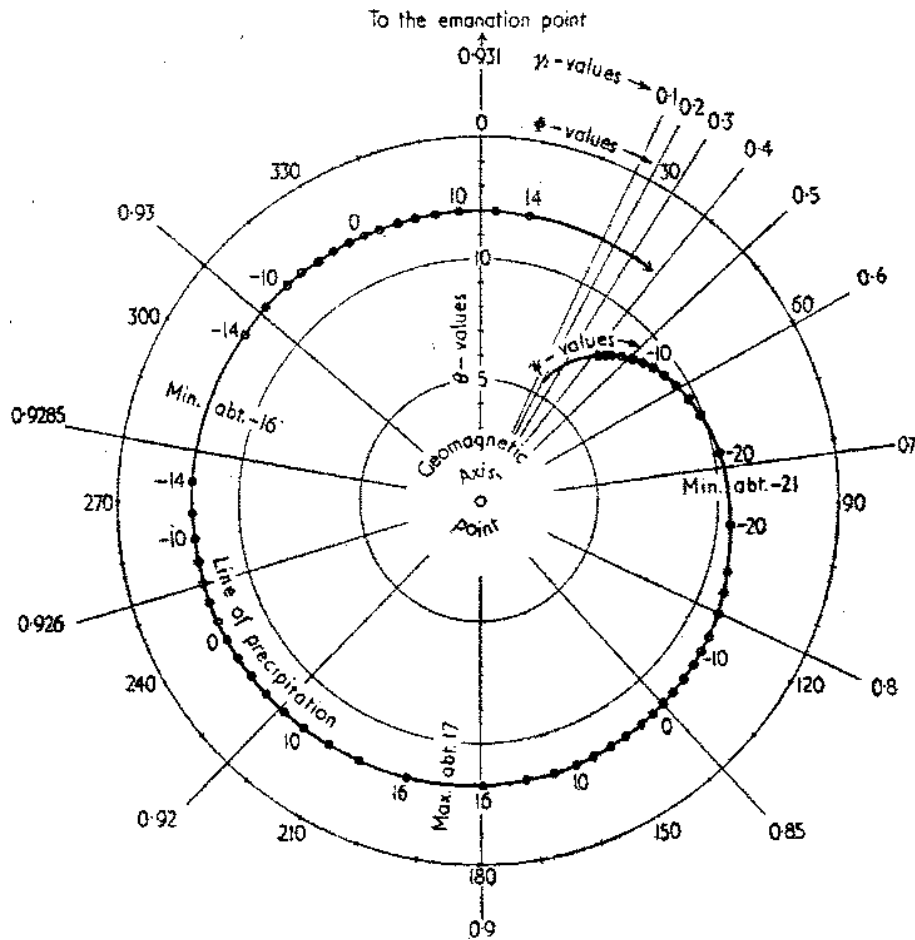


**Figure 1.** Spiral of positive corpuscles' precipitation around the magnetic axis. Here,  $\gamma$  stands for a constant of integration and  $\Psi$  is the declination of the sun (Størmer, 1955, Fig. 177).

107 ras. Protons of such energy precipitate, according to Størmer, 127  
 108 into a much smaller region than the polar latitudinal distances  
 109 of auroral features. Electrons with energy of a few eV, corre- 128  
 110 sponding to velocities of  $\sim 500 \text{ km/s}$ , would precipitate close 129  
 111 to the geomagnetic pole. However, their energy appears to be  
 112 too small to penetrate down into the upper atmosphere to a 130  
 113 level of  $\sim 100 \text{ km}$  above the Earth's surface, where discrete 131  
 114 auroral forms are usually seen (Harang, 1951). The results of 132  
 115 Størmer's theoretical calculations appeared to be applicable  
 116 to the particles of cosmic radiation, whose energy is several 133  
 117 orders of magnitude larger than those of the plasma fluxes, 134  
 118 which are responsible for the geomagnetic disturbances and 135  
 119 auroras. 136

120 In the following sections, we sum up the basic findings 137  
 121 concerning the spiral distributions in its historical progres- 138  
 122 sion, discuss the results of various authors, and in Section 6 139  
 123 we consider the relationship between the spirals and models 140  
 124 of the magnetospheric-ionospheric current systems. In the 141  
 125 Conclusions we list the basic steps in exploring the spiral dis- 142  
 126 tributions of geomagnetic variations and auroras and discuss 143

their place within the magnetospheric plasma structure.

## 2 Spiral distributions in regular ( $S_D$ ) geomagnetic field variations

2.1 The variations of the magnetic field  $D$ , which are observed at the Earth's surface during geomagnetically disturbed days are composed of various sources:

$$D = DCF + DR + DPC + DP + DT + Di \quad (1)$$

where  $DCF$  describes the field of magnetopause currents,  $DR$  the field of the ring current in the inner magnetosphere,  $DPC$  the field of the current system with the electrojet in the dayside cusp,  $DT$  the field of the cross-tail current and its closure magnetopause current,  $DP$  the field of elementary polar magnetic disturbances (substorms) with characteristic lifetimes of some tens of minutes to several hours, and  $Di$  the field of irregular oscillations of the geomagnetic field. The  $DP$  variations are referred to the substorm type variations ( $DP1$ ) only in the following.  $DP2$  variations are of different

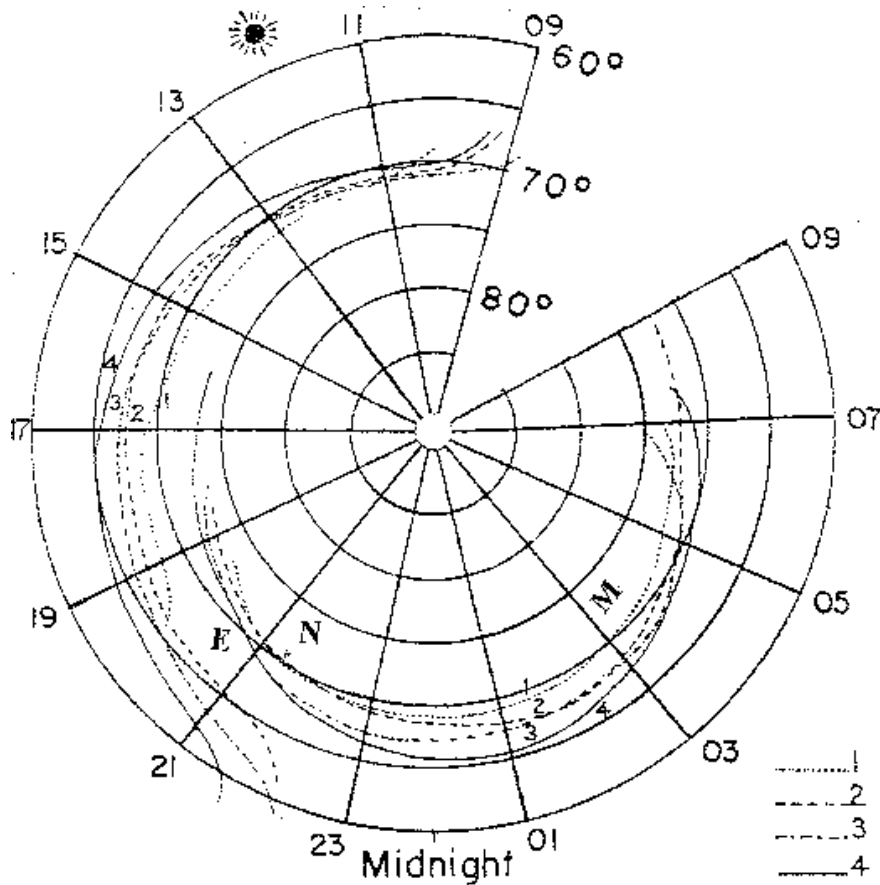


**Figure 2.** Loci of maximum intensity of auroral-zone electric currents (electrojets), as observed on geomagnetic meridian  $120^\circ$ , for different ranges of storminess (1,2,3,4). Mean picture for  $\Delta H$  and  $\Delta Z$  fields, letters M, N, and E correspond to morning, nighttime, and evening spirals (Harang, 1946).

144 nature and are not considered here. The  $DCF$ ,  $DR$ ,  $DPC$ , 164  
 145 and  $DT$  variations are significantly smaller than  $DP$  and  $Di$  165  
 146 at high latitudes on ground level, except for magnetic storm 166  
 147 intervals, so that one usually assumes: 167

$$148 \quad D = DP + Di \quad (2) \quad 168$$

149 Averaged over the international magnetic disturbance days, 170  
 150 one obtains the regular solar-daily variation field  $S_D$ , which 171  
 151 represents the integral effect of the polar disturbances  $DP$ . 172  
 152 The  $S_D$  variations are calculated as difference between the 173  
 153 hourly averaged values of the magnetic field elements for the 174  
 154 international disturbance days and the quiet days. 175

155 The current system obtained and named by Chapman as 176  
 156 solar-daily disturbed variation  $S_D$  has influenced the study 177  
 157 of geomagnetic disturbances to a high degree and became 178  
 158 the standard model. This was a major paradigm for a few 179  
 159 decades. The  $S_D$  current system consists of a pair of electro- 180  
 160 jets along the auroral zone as a circular belt with the centre 181  
 161 at the geomagnetic pole. The westward electrojet (WE) in 182  
 162 the morning sector and eastward electrojet (EE) in evening 183  
 163 sector are usually considered. On average, the WE has its 184

maximum intensity at 03.5 MLT, while the EE at 17.5 MLT (Allen and Kroehl, 1975).

The observations of the magnetic field variations were primarily of experimental character until the campaign of the Second International Polar Year (II<sup>nd</sup> IPY, 1932/1933). There were practically no permanent magnetic observatories at high latitudes by that time. The observations of high-latitude geomagnetic field variations by a network of magnetic stations during the II<sup>nd</sup> IPY period extended the possibilities of the researchers considerably. Based on observational material of the II<sup>nd</sup> IPY, Harang (1946) in Norway, Meek (1955) in Canada, and Burdo (1960) in the Soviet Union proposed models of polar magnetic disturbance current systems.

2.2 Harang (1946) used measurements of a chain of magnetic observatories along the  $120^\circ$  magnetic meridian from Spitzbergen (Svalbard) over Scandinavia till Potsdam to determine the  $S_D$  variations from three-component measurements of 11 observatories for four disturbance levels. He obtained so-called isopleths (lines of equal disturbance intensity) of these components.

2.2.1 Figure 2 shows the position of the maximum isopleths for all four magnetic disturbance levels. The diurnal variation of the isopleths' position is shown in the coordinates of geomagnetic latitude versus geomagnetic local time. The letters M, N, and E indicate segments of maximum isopleths, which researchers interpreted afterwards as morning (M), nighttime (N), and evening (E) spirals. The current flow is westward along the M and N spirals, but eastward along the E spiral. The isopleths run approximately parallel with the geomagnetic latitude for the H and Z components, and the maximal isopleths of the H component coincide with the auroral zone at  $67^\circ$  magnetic latitude. The H component within the auroral zone is positive during the evening hours (maximum at 17 MLT) and negative in the midnight to early morning hours (maximum intensity at 24–01 MLT) with a gap between the isopleths of opposite sign.

2.2.2 A characteristic Z component variation is observed at the auroral zone stations Tromsø ( $\Phi = 67.1^\circ$ ), Bossekop ( $\Phi = 66.6^\circ$ ), and Petsamo ( $\Phi = 64.9^\circ$ ): negative values are north of and positive to the south of the maximum H isopleths during the evening disturbance, and this reverses to the opposite during the nighttime disturbance. Throughout this paper,  $\Phi$  stands for geomagnetic latitude and  $\Phi'$  indicates corrected geomagnetic latitude. The significance of the distinction between  $\Phi$  and  $\Phi'$  consists in that to determine the deviation between the auroral zone and the geomagnetic parallel of  $67^\circ$  or, with other words, in the consideration of higher order harmonics of the internal potential sources, additional to the dipolar field (Hultqvist, 1958; Gustafsson, 1970). The curve for  $S_D$  in Z appears as a double wave. This double wave appears in all four disturbance levels. Assuming that the field of the magnetic disturbances is produced by a linear overhead current, it is evident that maximum values in  $\Delta H$  and a zero crossing in  $\Delta Z$  are located just below this current flow. This variation in  $\Delta H$  and  $\Delta Z$  in a certain distance from the line current is qualitatively in accordance with the isopleths. Between the evening and the nighttime isopleths at auroral latitudes ( $\Phi \sim 67^\circ$ ) exists therefore a longitudinal discontinuity, both in the variations of the magnetic field and in the current system of polar magnetic disturbances. Resulting from the existence of a discontinuity in the auroral zone, the zone itself consist of two separate branches. The discontinuity of the current system in the nighttime auroral zone causes the existence of the double wave structure in the Z component variations.

2.2.3 From the consideration of Figure 2 follows:

1. a shift of the maximum intensity current toward the equator with increasing disturbances;
2. the existence of a discontinuity in MLT for the isopleths at auroral latitudes in the midnight sector (discontinuity between E and N spirals);
3. the placement of the evening isopleths with an eastward current in the auroral zone latitudes over the whole in-

terval of 11–21 MLT;

4. the shift of the isopleths with westward current (M and N spirals) to higher magnetic latitudes from the midnight auroral zone both toward the morning and the evening hours;
5. in the evening hours there exists a latitudinal gap between the positive and negative isopleths (E and N spirals). The N spiral with the westward current is at higher latitudes than the E spiral. Harang didn't give due attention to the existence of the latitudinal gap but to a discontinuity at a fixed latitudinal distance near midnight. At the time of the publication (1946), there was a generally accepted paradigm about a auroral zone at  $\Phi \sim 67^\circ$  and about the position of electrojets along this zone (but not along the auroral oval yet unidentified at that time), so that he couldn't make an adequate conclusion about the nature of the gap between the electrojets.
6. Based on the close connection between the magnetic disturbances and the auroras and the existence of a local time discontinuity in the current system between the electrojets, Harang (1946) concluded, that the auroral zone should also consist of two parts with a discontinuity between them. The most intense auroras occur during 17–18 LT and 21 LT with a quiet period during the intermediate interval.
7. the currents producing polar magnetic storms as well the diurnal variations are most simply explained according to the dynamo theory (Harang, 1951).

2.3 Meek (1955), in his analysis of the magnetic field variations, uses data from all high-latitude geomagnetic observatories north of  $40^\circ$ , which participated in the  $II^{nd}$  IPY. Based on  $S_D$  variations, moments of the diurnal positive maximum of the disturbance vectors as well as their negative diurnal minimum were determined. Then a polar plot of magnetic latitude versus local geomagnetic time was made to display the diurnal maximum of the H component decrease for all stations. The points drawn lie along a spiral which expands clockwise (M spiral with westward current). The corresponding plot of the diurnal maximum of the H component increase shows a spiral expanding in the opposite direction (E spiral with eastward current). M and E spirals intersect on  $\sim 10$  a.m. (MLT) at  $\Phi \sim 70^\circ$  and on  $\sim 10$  p.m. at  $\Phi \sim 60^\circ$ . It is assumed that the magnetic spirals obtained are Størmer's spirals of precipitating particles from a plasma cloud arriving from the sun.

The spiral M expanding clockwise will be due to the precipitation of negatively charged particles, while the spiral E expanding anticlockwise due to positively charged particles.

2.3.1 The patterns of spirals with currents in the papers of Meek (1955) and Harang (1946) differ in the number of spirals, their positions, and with respect to their sources:

- 289 1. two spirals M and E, which form the oval of Meek 341  
290 (1955) versus three spirals M, E, and N at auroral lat- 342  
291 itudes of Harang (1946); 343
- 292 2. the spirals M and E intersect on 22 MLT at  $\sim 60^\circ$  lati- 344  
293 tude without any disruption according to Meek (1955), 345  
294 while there exist a discontinuity in MLT according to 346  
295 Harang (1946); 347
- 296 3. Meek relates the maximum decrease in the H compo- 349  
297 nent of the magnetic field along the M spiral with pre- 350  
298 cipitating electrons, and the maximum increase in the H 351  
299 component along the E spiral with proton precipitations 352  
300 (the sign of the charged corpuscles precipitating along 353  
301 the spirals oppose the sign of those in Størmer's calcu- 354  
302 lations). The winding of the spirals is therefore oppo- 355  
303 site to the assumption in the model of Størmer. For the 356  
304 explanation of the configuration of maximum isopleths 357  
305 (spirals), Harang utilises the dynamo theory of magnetic 358  
306 variations, and Meek the precipitating corpuscles; 359
- 307 4. after the midnight intersection of the spirals with west- 361  
308 ward and eastward currents, the westward current in the 362  
309 evening sector is positioned equatorward of the east- 363  
310 ward current according to Meek (1955), while it is pole- 364  
311 ward of the eastward current in the evening sector ac- 365  
312 cording to Harang (1946). 366

313 2.3.2 Meek (1955) modifies the opinions of Størmer by 368  
314 assuming the corpuscular solar flux as a plasma, but not as 369  
315 an ensemble of individual charged particles. It ensued just 370  
316 from such a modification, that electrons precipitate along the 371  
317 M spirals and protons along the E spirals. The westward 372  
318 electrojet ( $\Delta H < 0$ ) yields from the precipitation of electrons, 373  
319 while the eastward electrojet ( $\Delta H > 0$ ) is related to protons. 374

320 Assuming that the magnetic disturbance deviations are due 375  
321 to the motion of electric charges near the base of auroral 376  
322 forms, Meek (1955) expected some peculiarities in the dis- 377  
323 tribution of auroras, caused by the spiral distribution of max- 378  
324 imum intensities of magnetic variations and by particle pre- 379  
325 cipitations of different charges along the M and E spirals. 380  
326 The auroral luminosity configuration along the spirals allows 381  
327 the interpretation of some peculiarities of their morphology 382  
328 in the auroral zone and equatorward of it according to the de- 383  
329 scriptions in the literature: the diurnal variation of their oc- 384  
330 currence frequency; the motion during the evening and morn- 385  
331 ing hours; the orientation of the arcs; the appearance of auro- 386  
332 ras as due to separate precipitations of electrons and protons. 387

333 2.4. Based on data from 22 high-latitude observatories in 388  
334 the Northern Hemisphere with  $\Phi > 60^\circ$ , Burdo (1960) has 389  
335 shown that the diurnal variations of the disturbance inten- 390  
336 sity of the horizontal magnetic field components ( $\Delta T$ ) have 391  
337 2 or 3 maxima in dependence on the latitude. The positions 392  
338 of the maxima in ( $\Delta T$ ) within plots of MLT versus  $\Phi'$  (cor- 393  
339 rected geomagnetic latitude) are arranged in 3 groups: morn- 394  
340 ing (M), nighttime (N), and evening (E) points. The time 395

of maximum  $\Delta T$  changes with latitude for each group sep-  
arately. These changes are for all three groups practically  
linear in the orthogonal projection used here. This relation  
can be written as  $\Phi' = \Phi_0 + kt_m$ . In polar coordinates for a  
particular UT moment, this relation transforms into a part of  
a spiral with  $r = A + B\Lambda$ , where  $r$  is the distance (colatitude)  
of  $\Phi'$  from the pole,  $\Lambda$  is the geomagnetic longitude or the  
geomagnetic time, and A, B are constants. The  $\Delta T$  vectors  
are drawn onto this polar projection as arrows. Such a use  
of perturbing vectors as "current arrows" at a network of sta-  
tions gives a direct picture of the field distribution and was  
often applied by Birkeland.

2.4.1 The arrows cut the spirals under an angle near  $90^\circ$ .  
Numbers at the arrows' footpoint indicate the values of the  
vertical component of the disturbance vector  $\Delta Z$ . Each spi-  
ral sub-divides areas with positive and negative  $\Delta Z$ . The  $\Delta T$   
vector assumes therefore a maximum value along the three  
spirals at high latitudes with the direction perpendicular to  
the spirals and at the intersection points the vertical compo-  
nent  $\Delta Z$  of the disturbance vector changes its sign. Under  
the assumption that the horizontal current system constitutes  
the source of the magnetic disturbances, the spirals are the  
places of maximum current density. The direction of  $\Delta T$  and  
the sign of  $\Delta Z$  to both sides of the spiral determines the di-  
rection of the current along the spiral: along the morning  
and nighttime spiral the current is westward, while along the  
dayside spiral the current points eastward.

2.4.2 Burdo (1960) proposed that the dynamo-effect plays  
a notable (or even main) role in the generation of magnetic  
variations during disturbed time intervals. The currents pro-  
ducing the Sq variations and the polar magnetic disturbances  
are most simply explained according to the dynamo-theory  
proposed by Steward (1882). According to this theory the  
air in the upper atmosphere is ionised and thus electrically  
conducting. The tidal and other motions of the atmosphere  
will set up horizontal motion in the layers across the lines  
of force of the Earth's permanent magnetic field. Due to  
this electromotive forces will be formed, and electric cur-  
rents will be caused to flow in directions which agree with  
those required to produce Sq variations. The precipitation  
of electrically charged particles which produce the aurorae,  
strongly increases the ionisation and thus the conductivity  
of the ionized layers, which leads to cardinal changes of the  
high-latitude current system. This system of ionospheric cur-  
rents is - according to the dynamo theory - responsible for the  
generation of magnetic disturbances, so-called  $S_D$  variations,  
as well as for polar magnetic storms. Processes, which are  
generated in the ionosphere due to the penetration of corpus-  
cular fluxes, play the main role for the generation of magnetic  
disturbances. These fluxes enter the upper atmosphere at au-  
roral latitudes and a 2-D current system, which generates the  
magnetic disturbances, spreads out in the ionosphere.

2.5 The most exhaustive development of the dynamo the-  
ory, which is applicable to the magnetic field variations at  
high latitudes, was accomplished in the works of Japanese

396 scientists. Nagata and Fukushima (1952) and Fukushima 440  
 397 (1953) used the dynamo theory for the interpretation of two 441  
 398 specific types of the geomagnetic variations, which were 442  
 399 observed during the II<sup>nd</sup> IPY: a single-vortex current sys- 443  
 400 tem with the westward electrojet at auroral latitudes in the 444  
 401 nighttime sector, or a double-vortex system with westward 445  
 402 and eastward electrojets at auroral latitudes during the night- 446  
 403 time and evening hours, respectively. The conductivity is 447  
 404 steeply enhanced in the auroral zone (colatitude range of 448  
 405  $\Theta \sim 20^\circ \div 25^\circ$ ) during magnetic disturbances and stays at 449  
 406 the higher level of about one order of magnitude compared 450  
 407 with the polar region. The neutral wind in the conducting 451  
 408 layer depends on colatitude, longitude and the phase angle 452  
 409  $\alpha$ . The model current system can be brought in accordance 453  
 410 with the corresponding calculated magnetic field variations 454  
 411 by varying the input parameters of the model. In case of 455  
 412 enhanced conductivity in the auroral zone along all longi- 456  
 413 tudes, the model current system results in a double vortex 457  
 414 with westward and eastward electrojets. If the conductivity 458  
 415 is enhanced only within a limited longitudinal range, then the 459  
 416 model current system remains a single-vortex system with an 460  
 417 electrojet in those longitudes of enhanced conductivity. The 461  
 418 angle  $\alpha$  controls the direction of the current closure across 462  
 419 the polar cap.

420 2.6 Fukushima and Oguti (1953) considered the dynamo 463  
 421 theory with an anisotropic ionospheric conductivity. Under 464  
 422 several simplifying assumptions they obtained an expression 465  
 423 for the current function  $J_D$  in northern and southern auroral 466  
 424 zones, in the polar caps, and in the equatorial zone. 467

425 The current function has the form: 468

$$469 J_D = 2K_3^0 G k_1^1 \left\{ A_1 U_1(\Theta) \sin \lambda + B_1 U_1(\Theta) \cos \lambda \right\} \quad (3) 470$$

471 ... in the Northern polar cap 472

$$473 J_D = 2b K_3^0 G k_1^1 \left\{ \frac{(b-1)}{b} S_1^1(\Theta) \cos \lambda + \right. 474 \\ 475 [A_2 U_1(\Theta) + A_3 V_1(\Theta)] \sin \lambda + \\ 476 [B_2 U_1(\Theta) + B_3 V_1(\Theta)] \cos \lambda \left. \right\} \quad (4) 477$$

478 ... in the Northern auroral zone 480

481 where  $K_3^0$  represents the height-integrated ionospheric con- 482  
 428 ductivity in the polar cap during quiet times,  $G$  is the Earth's 483  
 429 magnetic field strength at the equator,  $k_1^1$  is the coefficient 484  
 430 of a spherical harmonic series for the potential field of the 485  
 431 ionospheric wind velocity,  $U_1(\Theta) = \tan \Theta/2$ ,  $V_1(\Theta) = \cot \Theta/2$ , 486  
 432  $S_1^1(\Theta) = \sin(2\Theta/4)$ ,  $A_1$ – $A_3$  and  $B_1$ – $B_3$  are numerical con- 487  
 433 stants, obtained from the boundary conditions, and  $b$ , finally, 488  
 434 is the enhancement factor of the conductivity in the auroral 489  
 435 zone during disturbed intervals in comparison with the quiet 490  
 436 time level. 491

437 2.7 The model current system reminds of the  $S_D$  current 492  
 438 system, though of a somehow smaller intensity, with two 493

electrojets in the auroral zone ( $65^\circ < \Phi < 70^\circ$ ) and its dis-  
 tributed currents in the polar cap ( $\Phi > 73^\circ$ ). The ionospheric  
 neutral wind system for the model calculation of  $S_D$  was  
 adopted analogous to the calculations of  $S_q$  variations. There  
 is a very essential difference between the observed and the  
 modelled  $S_D$  systems: the current direction in the polar cap  
 differs by an angle between  $110^\circ$  and  $150^\circ$ . This problem is  
 usually avoided in the dynamo theory by assuming different  
 neutral wind systems for the  $S_q$  and  $S_D$  variations at iono-  
 spheric altitudes (Nagata et al., 1950).

2.8 A series of articles of M. I. Pudovkin is devoted to  
 the use of the dynamo theory for interpreting the specifics  
 of the evolution of magnetic disturbances at high latitudes,  
 generalized in his thesis on “The morphology and nature of  
 polar magnetic storms” (Pudovkin, 1968). In these articles  
 the authors estimated the changes of the ionospheric con-  
 ductivity and deduced the neutral wind circulation at high  
 latitudes based on observations of geomagnetic field varia-  
 tions, of plasma densities, of drift velocities deduced from  
 plasma irregularities in the ionospheric E-layer, and from  
 movements of discrete auroral forms. It is assumed that cur-  
 rents, which cause the magnetic field variations, flow during  
 magnetic disturbances along extended auroral forms (arcs).

These currents are carried by the neutral wind away from  
 the arc and their position is determined from magnetic field  
 observations, while the direction and velocity magnitude of  
 the neutral wind in the ionosphere is calculated from the  
 direction and extent of the transport (Pudovkin, 1960; Pu-  
 dovkin and Evlashin, 1962). The current is usually shifted to-  
 ward south relative to the arc during positive disturbances (in  
 the evening) and toward north during negative disturbances  
 (nighttime to early morning hours). The velocity of the cur-  
 rent shift amounts to  $\sim 100$  m/sec. It is assumed that this shift  
 results from the action of neutral wind at ionospheric heights.  
 The sign of the geomagnetic disturbances in the horizontal  
 components is related to the direction of the causing cur-  
 rents: during positive disturbances the current shift toward  
 the equator and during negative toward the pole (Pudovkin,  
 1965b). For the determination of the wind velocity it is as-  
 sumed, that the source of ionization in the atmosphere (the  
 auroral arc) is static or moves only marginally for the distur-  
 bance time (Pudovkin and Korotin, 1961; Pudovkin, 1964).  
 The intensity of the magnetic disturbance is estimated from  
 the increase of plasma density as due to the interaction of  
 the corpuscular flux with the atmosphere and the velocity of  
 the neutral wind in the ionosphere (Korotin and Pudovkin,  
 1961). A considerable contribution comes also from iono-  
 spheric irregularities in the E-layer. Owing to the generation  
 of electric polarization fields, the velocity of the electrons in  
 the electrojets increases by an order of magnitude compared  
 to the neutral wind velocity. The Hall currents, which are  
 hereby generated along the auroral zone, appear to be the  
 cause for the observed magnetic field variations (Pudovkin,  
 1964).

2.9 Pudovkin (1965a) estimated the system of ionospheric neutral winds in the auroral zone from magnetograms and plotted it according to the longitude of the stations. At all stations in the evening hours the neutral wind is directed from north to south, while in the nighttime and early morning hours it is oppositely directed from south to north. The course of the  $S_D$  variations is controlled by the diurnal variation of the ionospheric neutral wind in such a manner that the currents, which are the cause for the  $S_D$  variations, are generated due to the dynamo action of the ionospheric neutral winds. The neutral wind system is comparatively stable according to the dynamo theory and experiences only a small variation, but the magnetic disturbances are caused by steep enhancements of the ionospheric conductivity due to the precipitating corpuscular fluxes (Pudovkin, 1965b). Based on the discussion of ionospheric processes, Pudovkin (1964, 1965b) concluded, that the dynamo theory is the best substantiated theory to explain the generation of ionospheric currents that are responsible for the high-latitude magnetic disturbances. These currents are excited due to the dynamo action of ionospheric neutral winds.

2.10 Viewed from the vintage point of the present, it is amazing how broadly and deeply the success of the dynamo theory was in interpreting the quiet-time features of the ionosphere. But the application of the dynamo theory as physical base to interpret the nature of the geomagnetic disturbances at high latitudes encountered distinct difficulties, both in observational as in theoretical respects. We already mentioned above the discrepancies in the results of the classical dynamo theory with regard to the phase and intensity of the observed current systems, both in magnitude and direction (phase) within the polar cap. The modifications of the theory by M. I. Pudovkin were also not without any problems as listed subsequently.

1. The assumption about the static behaviour of the corpuscular source (auroral arc), which is used for the determination of the neutral wind velocity at ionospheric heights, disagrees with present perceptions of the dynamics of discrete auroral forms. In the majority of cases the auroras appear and allocate not at a fixed latitude, but along the auroral oval, which is asymmetric with respect to the geomagnetic pole. In consequence of this there is a shift of the aurora with  $\sim 30$  m/sec from north toward south in the evening and from south toward north in the morning. During substorm creation (growth) phases, the arcs in the evening–nighttime sector are shifted with a velocity up to  $\sim 250$  m/sec southward. This is just the same range of velocities as that of the neutral wind velocities in the modified dynamo theory.
2. The magnetic variations at auroral zone latitudes ( $\Phi \sim 67^\circ$ ) in the evening sector are positive and, therefore, in the frame of the dynamo theory, the neutral wind in the

ionosphere should be directed from north to south. In the same sector at latitudes of the auroral oval ( $\Phi \sim 70^\circ$ ), the magnetic variations are negative and consequently the neutral wind should be directed there from south to north. This divergence of the neutral wind orientation within close latitudinal distances at the evening sector suggests the presence of a neutral wind source within this small latitudinal range. But the existence of such a source is not envisioned in the frame of the dynamo theory.

3. The current system in the dynamo theory is a 2-D one, spanning at the ionospheric E-layer. According to present conceptions, based on experimental data, the current system of the magnetic disturbances is 3-D. The ionospheric electrojets are connected by field-aligned currents (FACs) with the magnetosphere. The character and the intensity of the magnetic disturbances at the Earth's surface is determined by a complicated system of ionospheric and magnetospheric currents.
4. Nowadays it is generally accepted, that the magnetic disturbances at high latitudes as well as the currents in the magnetosphere and ionosphere, which cause them, are controlled by the parameters of the interplanetary medium. The dominating parameter here appears to be the orientation and intensity of the interplanetary magnetic field (IMF), in combination with the solar wind velocity.

2.11 New approaches for the determination of the upper atmosphere neutral wind system at high latitudes were established during the “Sputnik era”. It became possible to determine the velocity and direction of the neutral wind in situ in the thermosphere. The satellite Dynamics Explorer–2 (DE–2) measured the velocity of the neutral wind at altitudes between 300 km and 550 km by use of an Fabry-Perot interferometer and a wind and temperature spectrometer (Killeen and Roble, 1988). The empirical neutral wind pattern obtained in geomagnetic coordinates is characterised by a strong antisolar flow over the geomagnetic pole bordered by sunward flow in the dawn and dusk sectors. Negative vorticity occurs in the dusk sector while positive vorticity in the dawn sector.

Measurements of lower thermospheric neutral winds at altitudes between 100 km and 300 km, where according to the dynamo theory ionospheric currents are generated, have been realized onboard the Upper Atmosphere Research Satellite (UARS). Richmond et al. (2003) used data of the Wind Imaging Interferometer (WINDII), which records the line-of-sight intensity of the green atomic oxygen line airglow emissions. They showed that the neutral wind motion is controlled by the IMF action down to 105 km altitude, while above  $\sim 125$  km the wind patterns shows considerable similarity with the ionospheric convection patterns. The correlation between the IMF  $B_z$  component and the diurnal har-



600 monic of the neutral wind is best, when the IMF is averaged 655  
 601 over the preceding 1.0÷4.5 hours. Zonal wind below 120 km 656  
 602 correlates with the IMF  $B_y$  component when the  $B_y$  compo- 657  
 603 nent is averaged over the preceding 20 hours. Above 120 km, 658  
 604 the dusk side clockwise circulation wind cell is prominent 659  
 605 and it intensifies for IMF  $B_z < 0$ . Around 120 km one ob- 660  
 606 serves a dawn side anticlockwise wind cell that responds to 661  
 607 IMF  $B_z$  variations. During intervals with IMF  $B_z > 0$ , the 662  
 608 neutral wind modification is mainly confined to the polar 663  
 609 cap, while for  $B_z < 0$  it extends to subauroral latitudes. On 664  
 610 timescales of  $\sim 20$  hours an IMF  $B_y$  dependent zonal wind 665  
 611 generally exists at 120 km altitude and  $80^\circ$  geomagnetic lat- 666  
 612 itude with maximum wind speeds of  $\sim 60$  m/s. The paper 667  
 613 of Richmond et al. (2003) includes a broad range of refer- 668  
 614 ences on thermospheric neutral wind investigations and their 669  
 615 modelling. 670

616 Cross-track accelerometer measurements at the CHAMP 671  
 617 satellite were used to deduce statistical neutral wind pat- 672  
 618 tern at the high-latitude upper atmosphere (Lühr et al., 2007; 673  
 619 Förster et al., 2008). These measurements were obtained at 674  
 620 altitudes of  $\sim 400$  km and confirmed the existence of a strong 675  
 621 antisolar flow with an average velocity of  $\sim 500$  m/s and an 676  
 622 azimuth of  $168^\circ$  over the central polar cap. At the evening 677  
 623 side a large clockwise circulation cell is formed, resulting 678  
 624 in the tendency for westward (sunward) neutral wind veloc- 679  
 625 ities in the auroral region of the duskside upper atmosphere. 680  
 626 Förster et al. (2008, 2011) analysed the neutral wind obser- 681  
 627 vations of CHAMP in dependence on the IMF orientation. 682  
 628 The data were sorted into 8 separate IMF sectors with  $45^\circ$  683  
 629 width each. Measurements over a 2-year interval resulted in 684  
 630 a good data coverage for each IMF sector. The upper ther- 685  
 631 mospheric neutral wind system is characterized in all sectors 686  
 632 by a transpolar neutral wind orientation across the central 687  
 633 polar cap and two vortex cells with opposite circulations on 688  
 634 the dawn and dusk side, the strength and shape of which de- 689  
 635 pend on the IMF  $B_y$  and  $B_z$  components. The amplitude of 690  
 636 the cross-polar cap neutral wind flow is largest for negative 691  
 637 IMF  $B_z$  values ( $B_z < 0$ ) and amounts on average to  $\sim 570$  m/s 692  
 638 (cf. Förster et al., 2008, Table 1). A couple of characteristic 693  
 639 phenomena of the IMF  $B_y$  and  $B_z$  dependence on the spatial 694  
 640 distribution of the neutral wind in the upper atmosphere are 695  
 641 gathered and described in detail. 696

642 The satellite observations of thermospheric neutral wind 697  
 643 and ionospheric plasma convection revealed a fairly close 698  
 644 similarity of their patterns. The correlation of the velocity 699  
 645 and direction of the neutral wind and plasma convection with 700  
 646 the IMF  $B_z$  and  $B_y$  components verifies the control of the 701  
 647 thermospheric neutral wind regime by the IMF parameters. 702  
 648 Both the plasma motion and the neutral wind appear as a 703  
 649 result of the electric fields, generated in the outer magneto- 704  
 650 sphere. They are constituted due to the interaction of the 705  
 651 solar wind with the geomagnetic field and then transmitted 706  
 652 along the magnetic field lines down into the ionosphere. The 707  
 653 plasma in the thermosphere drifts in the electric and mag- 708  
 654 netic fields. The neutral thermospheric component adopts the 709

plasma motion due to the ion drag forces. The secondariness  
 of the neutral wind results in a time lag of the neutral wind  
 with respect to the convection. The magnitude and direction  
 of the ion motion is determined by the intensity of the IMF  
 components. Due to these relations, the neutral wind at high  
 latitudes also depends on the IMF.

The global neutral wind system, that is due to this interac-  
 tion, differs considerably from that system, which is essential  
 for the generation of magnetic disturbances observed at the  
 Earth's surface, as explained by the existing dynamo theory.

2.12 Patterns of magnetic disturbance spirals, that were  
 obtained from the materials of the II<sup>nd</sup> IPY by L. Harang,  
 J. H. Meek, and O. A. Burdo, differ both in the quantity of  
 spirals and in their sources (2 spirals of corpuscular precipi-  
 tation according to J. H. Meek, but 3 spirals in the dynamo  
 theory according to L. Harang and O. A. Burdo). All three  
 studies used yearly averaged data. There are, however, sig-  
 nificant seasonal dependences in the variations on the geo-  
 magnetic field (Benkova, 1948; Feldstein, 1963a). Feldstein  
 and Zaitzev (1965a) studied the  $S_D$  variations of three geo-  
 magnetic field components using data of 24 magnetic obser-  
 vatories during the IGY of the Northern Hemisphere separ-  
 ately for winter, equinox, and summer periods. The horizon-  
 tal projection of the disturbance vector  $\Delta T$  was determined  
 according to the relation  $\Delta T = \sqrt{(\Delta H^2 + \Delta D^2)}$  as deviations  
 from the quiet time level with  $\Delta D$  as the deviation from the  
 East-West component.

2.12.1 During the winter season, the  $S_D$  variation at  $\Phi' >$   
 $73^\circ$  is characterized by one maximum near midday. In the  
 latitude range  $73^\circ > \Phi' > 67^\circ$  the maxima of  $\Delta T$  occur in the  
 evening and morning hours, and in the latitude range  $67^\circ >$   
 $\Phi' > 60^\circ$  they shift to nighttime and evening hours. Below  
 $\Phi' < 60^\circ$  the nighttime maximum in  $\Delta T$  is the only one.

Figure 3a shows the patterns of  $\Delta T$  and  $\Delta Z$  for the winter  
 season of the IGY (November 1957 – February 1958) in co-  
 ordinates of  $\Phi'$  versus MLT. The arrows indicate the distur-  
 bance vector directions in the horizontal plane; the arrow's  
 length is in accord with the amplitude of  $\Delta T$ . The scale is  
 given in the upper left corner of the Figure. The numbers  
 at the arrow's origin specify the amplitude of  $\Delta Z$ . The de-  
 pendence on the maximum moments in the course of the di-  
 urnal variation of  $\Delta T$  over  $\Phi'$  is indicated with thick lines:  
 (1) – morning maximum (M), (2) – nighttime maximum (N),  
 and (3) – evening maximum (E) in Fig. 3a. The sign of the  
 $Z$ -component of the geomagnetic variations changes along  
 these lines. Such a distribution of the vector magnitude and  
 direction implies, that intense equivalent currents are flow-  
 ing along these lines. Along the lines 1 and 2, forming an  
 oval belt, the current flows westward and decreases the hori-  
 zontal magnetic component. Along line 3 the current flows  
 eastward, increasing this component.

2.12.2 In the limited latitudinal range of  $69^\circ < \Phi' < 72^\circ$ ,  
 there exist only negative disturbances of the horizontal com-  
 ponent during the whole day. This region at auroral lati-  
 tudes, where we have  $\Delta H < 0$  in the winter season during

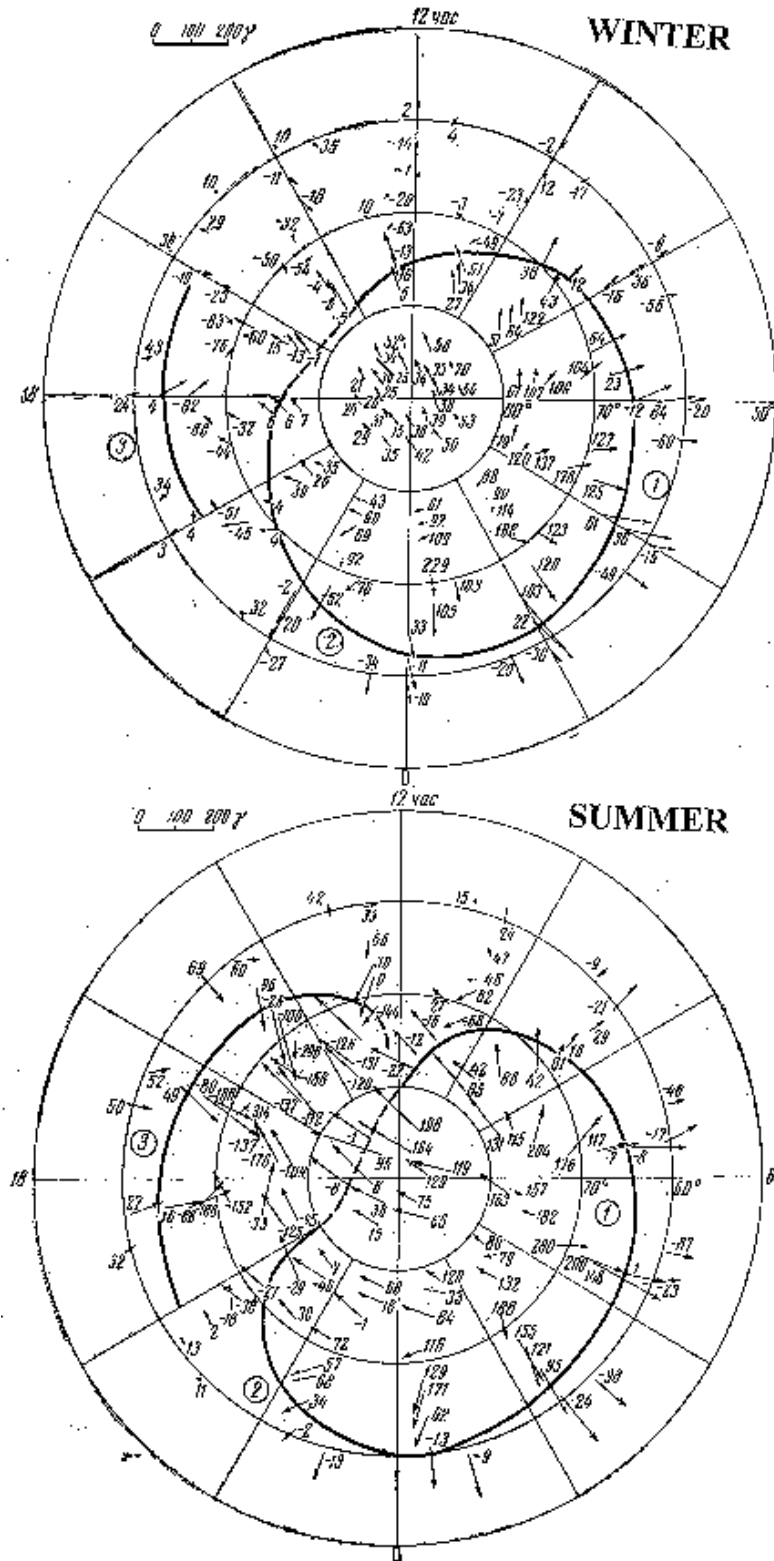


**Figure 3.** Loci of maximum intensity  $\Delta T$  and minimum  $\Delta Z$  fields in LMT versus corrected geomagnetic latitudes in Northern Hemisphere. The digits 1, 2, and 3 correspond to morning, nighttime, and evening spirals, respectively (Feldstein and Zaitzev, 1965a). a) winter season of IGY (upper panel) and b) summer season of IGY (lower panel).

the whole day, is fundamentally different from the character of the diurnal variation within the auroral zone. There occur beside the disturbances with  $\Delta H < 0$  during the nighttime and morning MLT hours generally at the same UT also disturbances  $\Delta H > 0$  in the evening MLT hours (Burdo, 1960). The existence of a latitude interval with  $\Delta H < 0$  was confirmed by the observations of the drifting station North Pole  $66^{\circ} < \Phi' < 70^{\circ}$  during the period from September 1957 to April 1958 (Zhigalova and Ol, 1964). During all hours of the day, they practically observed only negative bays. The frequency of their appearance maximizes at 07 and 21 MLT, which corresponds to the times of the station's passage under the oval current belt (Fig. 3a, lines 1 and 2) in the course of the Earth's rotation. The current belt at Fig. 3a, which consists of the spirals 1 and 2, coincides with the position of the auroral oval (Feldstein, 1963b, 1966), Auroras were observed along the auroral oval during the winter season of the IGY practically continuously at zenith. The appearance of discrete auroral forms implies the precipitation of energetic electrons into the upper atmospheric layers. The electron precipitation with energies of  $1 \div 5$  keV along the auroral oval leads to steep increase of the conductivity at dynamo region altitudes. The incoming and outgoing FACs result in the generation of a meridional electric field, directed equatorward. In this way the conditions for the appearance of the electrojet with a westward directed Hall current are established along the auroral oval.

2.12.3 Fig. 3b shows the patterns of  $\Delta T$  and  $\Delta Z$  for the summer season of the IGY in coordinates of  $\Phi'$  versus MLT. The legend here is the same as for Fig. 3a. The dependencies of the maximum moments in the course of the diurnal variation of  $\Delta T$  are depicted with the thick lines 1(M), 2(N), and 3(E), together with the corresponding sign changes of  $\Delta Z$ . The M and N spiral with negative values of  $\Delta H$  forms, as in the winter season, the auroral belt, along which the current flows in westward direction. In contrast to the winter season,  $\Delta T$  increases sharply in daytime hours at  $\Phi' > 75^{\circ}$ . The intensity of the disturbances in the dayside sector at the auroral oval is comparable with the nighttime–early morning disturbances at latitudes of the auroral zone. A noticeable increase of the  $\Delta T$  vector intensity, caused by the positive values of  $\Delta H$ , occurs during evening MLT hours in the range  $60^{\circ} < \Phi' < 70^{\circ}$ . The patterns of  $\Delta T$  and  $\Delta Z$  for the summer and winter seasons during the IGY give no hint on the existence of two circular zones at fixed latitudes with maxima of the magnetic activity. The absence of such circular zones is confirmed by latitudinal cross-sections in  $\Delta T$  during various MLT hours.

### 3 Spirals in the irregular geomagnetic field variations $D_i$ (agitation)

3.1 The high-latitude diurnal geomagnetic variations contain a component, which displays an irregular character. It is usu-

ally investigated by studying the regularities of geomagnetic activities. Mayaud (1956) proposed the term agitation for the indication of geomagnetic disturbances, which are due to the precipitation of corpuscular radiation into the upper atmosphere, leading to irregular magnetic field variations. The intensity of agitation is estimated by means of various indices, which characterize the magnetic activity in different regions of the globe.

3.1.a The Polar Cap (PC) index is the most representative one for the polar cap, both for the Northern (PCN) and the Southern (PCS) Hemisphere (Troshichev et al., 1988, 2006). The PC indices are derived from ground geomagnetic measurements in the Northern (PCN) and Southern (PCS) Polar Caps. The PCN index is based on the data from Thule (Greenland) while the PCS index is based on data from Vostok in Antarctica. The PC index in its present form was first formulated by Troshichev et al. (1988) as a planetary index. PCN index values have been supplied from the Danish Meteorological Institute (DMI) while PCS index values have been supplied from Arctic and Antarctic Research Institute (AARI) (Troshichev et al., 2006). Basically, the PC index with a temporal resolution of 1 min represents the polar cap magnetic variations  $\Delta F_{PC}$  in  $nT$ , associated with the transpolar part of the current system driven by the electric field of the solar wind–magnetosphere dynamo.

3.1.b The planetary indices AE, AU, and AL were introduced by Davis and Sugiura (1966) to characterize the UT variation (in  $nT$ ) of the eastward (AU), the westward (AL) and the total electrojet intensity (AE). These indices were determined by the World Data Center A for Solar-Terrestrial Physics, NOAA, Boulder, USA (Allen et al., 1974, 1975) from 1966 to 1971. The indices were determined with a temporal resolution of 2.5 min as maximal deviation from the quiet time level for positive (AU) and negative (AL) values of the H-component of the geomagnetic field based on a network of 10–11 magnetometer stations. These observatories were distributed at auroral latitudes with a rather good coverage in longitude (Allen and Kroehl, 1975). During the subsequent years up to now, the AE, AU, and AL indices are determined with a 1-min cadence by the World Data Center for Geomagnetism, Kyoto, Japan, based on the data of 12 observatories.

3.1.c For the study of the regularities of agitation developments at high latitudes, one-hour amplitude averages of the horizontal components of H and/or D were largely employed (cf., e.g., Nikolsky, 1951; Burdo, 1960; Lassen, 1963, and references therein). Nikolsky (1947) used the curve-length of the D-variometer records as an every-hour characteristic of magnetic disturbances.

3.1.d Disturbances at mid-latitudes were estimated for particular geomagnetic observatories by means of the quasi-logarithmic index K (Bartels et al., 1939). This agreed measure, with values from 0 to 9, estimates the amplitudes of the H and D component variations as deviations from the quiet time level within 3-hourly intervals of UT. The estimation of

817 K indices in various observatories for one and the same time 872  
818 interval results generally in different values. 873

819 The averages of the K values from 11 different observa- 874  
820 tories within the latitudinal range of  $44^\circ < |\Phi| < 57^\circ$ , from 875  
821 which only one is localized at the Southern Hemisphere, re- 876  
822 presents the planetary index Kp. This index was introduced 877  
823 by Bartels in 1949. The Kp values counted according to a 878  
824 particular scale, translate to the equivalent 3-hourly ampli- 879  
825 tude index ap (in nT) and their daily averages Ap. The in- 880  
826 dices Kp, ap, and Ap were derived by the Geophysical In- 881  
827 stitute of the Göttingen University from January 1932 un- 882  
828 til the end of 1996. Since January 1997 the derivation and 883  
829 distribution of the Kp values have been moved to the Adolf 884  
830 Schmidt Geomagnetic Observatory Niemegk, part of the 885  
831 GeoForschungsZentrum (GFZ) Potsdam (now: GFZ German 886  
832 Research Centre for Geosciences, Helmholtz Centre Pots- 887  
833 dam). 888

834 To characterize the value of the daily magnetic activity 889  
835 level, the indices C and Ci are used. The magnetograms of 890  
836 any observatory are quantified for each day (in UT) with a 891  
837 magnetic character figure of the value 0, 1, or 2. This char- 892  
838 acter figure appears also as the C index of this day for the 893  
839 given observatory. Arithmetic mean values of the C index 894  
840 values from all reporting observatories result in the Ci index, 895  
841 which runs from 0.0 for very quiet conditions to 2.0 for very 896  
842 disturbed ones. The planetary index Cp for the daily distur- 897  
843 bance characteristic, which varies from 0.0 to 2.5 in steps of 898  
844 0.1, is calculated from the Ap index. The Cp index is used to 899  
845 discern the international magnetically disturbed and magnet- 900  
846 ically quiet days. 901

847 Mayaud (1967) assumed that the Kp index does not suf- 902  
848 ficiently reflect the planetary character of a magnetic distur- 903  
849 bance and proposed its modification. The modified indices 904  
850 Km, am, and Am are based on the K index of 24 mid-latitude 905  
851 stations, including 9 at the Southern Hemisphere. 906

852 3.1.e Magnetic disturbances of more than 100 years are 907  
853 described with the aa index (Mayaud, 1972). This index 908  
854 was calculated from the K index of the observatories Mel- 909  
855 bourne and Greenwich (i.e., one station in each hemisphere), 910  
856 beginning from 1868. Later these stations were replaced by 911  
857 Abinger and Hartland for Greenwich and by Toolangui and 912  
858 Canberra for Melbourne. From the aa values, daily means (Aa 913  
859 index) and monthly means are calculated. 914

860 3.1.f To describe the variations of the Earth's magnetic 915  
861 field during geomagnetic storms, the planetary Dst index is 916  
862 broadly used. A starting point for the studies concerning Dst 917  
863 derivation can be found at the end of the forties of the last 918  
864 century. More systematic determinations started after the 919  
865 IGY (Sugiura, 1964). For the derivation of the hourly Dst 920  
866 values, one usually uses hourly UT values of the low-latitude 921  
867 magnetic observatories Honolulu (USA), Kakioka (Japan), 922  
868 Hermanus (SAR), and San Juan (USA). These observatories 923  
869 were chosen for the reason that their locations are sufficiently 924  
870 distant from the auroral and equatorial electrojets and that 925  
871 they are distributed in longitudes as evenly as possible. The 926

Dst index represents the axially symmetric part of the dis-  
turbance magnetic field at the dipole equator on the Earth  
surface (in nT). Nowadays the World Data Center for Geo-  
magnetism, Kyoto, Japan, provides with 1-min resolution the  
so-called SymH index (replacing Dst) as well as an asymmet-  
ric index AsymH as difference between the maximum and  
minimum values of the H component from a network of low-  
latitude stations.

3.1.g Up to the nineties of the past century, i.e. practi-  
cally over 50 years, it was generally assumed, that during  
geomagnetic storms the Dst index represents the magnetic  
variation fields of the magnetopause currents DCF and of  
the ring current DR (see, for instance, the reviews of Gon-  
zalez et al., 1994; Kamide et al., 1998). The contribution of  
the magnetospheric tail current fields (DT) were assumed to  
be less than a few nT in the observations at the Earth's sur-  
face. Only resulting from the studies of Arykov and Maltsev  
(1993); Arykov et al. (1996); Alexeev et al. (1996); Maltsev  
(2004) it became clear, that the DT contribution in the Dst in-  
dex during magnetic storm periods is comparable to the DCF  
and DR contributions.

3.1.h The Sa (used in the literature to identify the diurnal  
change of geomagnetic activity) has a complicated form at  
high latitudes, which changes with latitude. The consider-  
ation of irregular magnetic disturbances revealed, that they  
follow certain regularities at particular stations, i.e. the mag-  
netic disturbance has a significant diurnal course. The on-  
set time as well as the maximum intensity of the disturbance  
depends on the station's position with respect to the auroral  
oval. Below we present, according to our guess, basic results,  
summarizing the research on magnetic agitation regularities  
at high latitudes concerning the spiral distributions. We seek  
to follow in this review the historical progression according  
to the publication time of new ideas.

3.2. The first study on Sa at high latitudes was performed  
with observational material of the II<sup>nd</sup> IPY by Stagg (1935),  
carried out with data of six arctic, one mid-latitude, and  
three antarctic stations. It was shown, that the form of Sa  
is determined by the magnetic latitude and local time. In  
mid-latitudes the activity maximizes during evening hours  
of local time. Progressing to higher latitudes, the maximum  
moves to later hours and during midnight it is observed at  
 $\Phi \sim 69^\circ$ . The form of Sa changes at latitudes of highest activ-  
ity between  $70^\circ < \Phi < 78^\circ$ . There two maxima are observed:  
one at the morning hours, the other during nighttime. At  
 $\Phi > 78^\circ$ , the maximum activity reaches morning or even mid-  
day hours. Nikolsky (1947) assembled observational results  
of 16 stations, partly positioned within the formerly inacces-  
sible Eastern regions of the Arctic, and found some differ-  
ences from Stagg's results: the morning maximum for sta-  
tions along one and the same geomagnetic parallel occurs at  
different local times; the equatorial boundary of the active  
zone is recorded down to a latitude of  $\Phi \sim 62^\circ$ ; the morning  
maximum appears in the western hemisphere almost con-  
currently at 15.5–16.5 MLT, while its appearance lags by

0.7 hours in the eastern hemisphere with  $\Phi$  shifted by  $1^\circ$ ; intensity variations with latitude are different during nighttime and morning maxima. Noting the differences of the evening and morning magnetic activities, Nikolsky (1947) assumed, that their behaviour follows different regularities. He didn't even exclude different natures of the corpuscular fluxes, responsible for the two types of magnetic disturbances.

3.3 Benkova (1948) considered 17 Arctic observatories and concluded, that the Sa value of high-latitude stations follow the scheme, that was proposed by Stagg (1935). The description of Sa as expansion of harmonic series according to

$$Sa = \sum_n C_n \cos(nt - \alpha_n) \quad (5)$$

has shown, that over the range of  $\Phi = 0^\circ$  to  $90^\circ$  the parameter  $\alpha_1$  varies between  $-2\pi$  and  $+2\pi$  and the sign change of the first term of the expansion occurs at the latitude of the auroral zone. The dependence on  $\alpha_1$  from  $\Phi$  in polar coordinates turns out to be a spiral, winding up in clockwise direction through the morning sector. This appears to be the first mention of a spiral distribution in the literature relating to the morning maximum of magnetic activity.

3.4 A.P. Nikolsky addressed the analysis of spiral distributions of the high-latitude magnetic activity in a large number of publications. The most important results are collected in the anthologies of the Arctic and Antarctic Research Institute (AARI) in St. Petersburg (Nikolsky, 1951, 1956, 1960a). It was shown, that the specific characteristic of the Sa consists in the appearance of maxima at morning, daytime, and nighttime hours, the relative amplitude of which varies in dependence on the stations's distribution. The intensity of the morning and dayside disturbances increases with increasing geomagnetic latitude, the nighttime disturbances are fixed to the local midnight and maximize at latitudes of the auroral zone. A.P. Nikolsky turned his particular attention to the study of morning and daytime disturbances. Considering observations at 30 places with  $\Phi > 60^\circ$ , the observational material is very broadly scattered about the indices of activity used. It turned out that the agitation during morning and daytime hours is not connected with the auroral zone. Considering contour maps of concurrent appearance (with respect to UT) of the morning agitation maxima, it became clear, that the isoline represent a system of spiral sections, which begin at the pole of homogeneous magnetization. At the Northern Hemisphere they wind up clockwise. Nikolsky assumed, that these sections of spirals should be seen as projections onto the Earth's surface of those real trajectories, along which solar corpuscles penetrate into the upper atmosphere. The positions of the most frequent particle precipitations along the spirals are determined by the character and the parameters of the particles in the corpuscular fluxes.

3.5 Nikolsky (1960a) identifies the spirals of the morning agitation maximum with the Størmer's spirals of penetrating solar corpuscles. Because these spirals wind up clockwise

in the Arctic, these corpuscles should be protons according to Størmer's theory. The appropriateness of Nikolsky's assumption about the congruency of his spirals with the spirals of Størmer was challenged by Agy (1960). He paid attention to the fact, that the Nikolsky's spirals of the morning Sa maximum represent positions at the Earth's surface of the simultaneous (in UT) onset moment of maximum activity along the whole spiral. These spirals differ essentially from those of Størmer, along which the penetration of corpuscles occurs simultaneously only in a few points. The whole spiral of Størmer results from corpuscular precipitations over a longer time interval of the order of a year.

3.6 Based on the calculation results of Størmer (1955), Nikolsky (1960a) concludes, that there exist four regions within the morning spirals, where the solar proton trajectories are gathering closer (see Fig. 1). These regions ("A", "B", "C", and "D") occur at 02, 08-09, 14, and 20 hours LT, respectively. Nikolsky suggests that as the Earth rotates diurnally under the spiral, the high point density sections of the spiral on Fig. 1 will trace out four ring "auroral zones" or regions with auroras in the zenith and increased magnetic agitation. In Fig. 1 there are four such high point-density sections and therefore, according to Nikolsky, four auroral zones will occur. Fig. 4 from the paper of Nikolsky (1960a) shows the positions of all four regions "A", "B", "C", and "D" at the Earth's surface. The figure shows also the image replication of Størmer's spiral (named "S"), the position of which was arbitrarily changed by Nikolsky. The spiral in Fig. 4 is prolonged to low latitudes (observatory Bombay in India). The extension of each of the "auroral zones" to the equator is limited by the position of the high point density section of the spiral in Fig. 4.

3.7 Zone "B" is identified as second (inner) region, where the intensity of magnetic agitation and the occurrence of auroras achieves maximum values at 08-09 LT. The summary effect of the precipitation zones "A" (02 LT) and D (20 LT) appears as the main auroral zone ("Fritz zone"), which is located at mid-latitudes over the American continent. Such a position of the "Fritz zone" is quite unusual and in case of its observational confirmation it would be a good argument in favour of the planetary distribution of corpuscular precipitation and the related auroras and magnetic agitation, as suggested by A. P. Nikolsky. Unfortunately, it is not possible to verify the appearance of zenith auroral forms in region "C" with observations - due to daylight conditions around 14 LT.

The appearance of auroral forms in the zenith discloses, in contrast to the magnetic disturbances, directly the location of precipitating corpuscular fluxes. Feldstein (1963a) verified hence the existence of four zones of maximum corpuscular precipitation using auroral observations from the IGY period (Annals, 1962).

3.8 The appearance of auroras is usually very rare at mid-latitudes and if it appears, then preferably with northern azimuths. Near the zones "A" and "D", in case they are precipitation zones, the auroral forms should appear mainly at

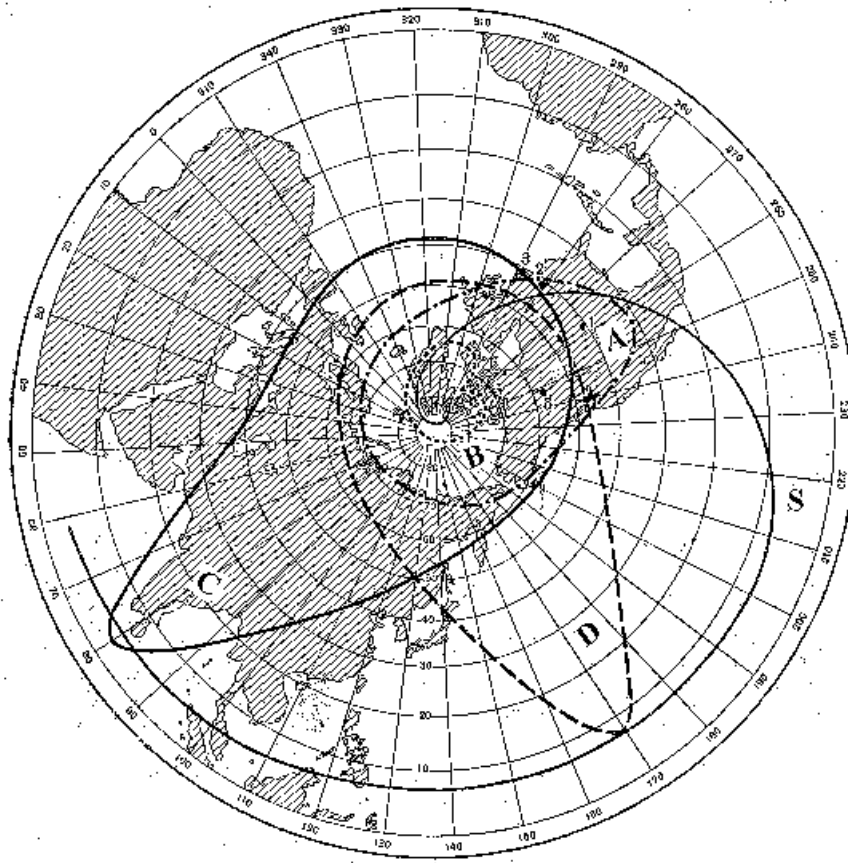


**Figure 4.** Location of solar corpuscular flux precipitation zones “A”, “B”, “C”, and “D” above Earth’s surface and corresponding maximum values of agitation and appearance frequency of auroras according to Nikolsky (1960a). Letter “S” marks Størmer’s spiral, which is arbitrarily prolonged towards low latitudes.

zenith. The positions of some observatories in the environment of zones “A” and “D” are shown in Fig. 4 and their coordinates are given in Table 1 together with the respective probability for the appearance of auroras in the zenith per cent of the total number of observations as well as the number of observation intervals with auroras northward and southward of the station.

From Table 1 follows, that the probability of zenith auroras at the stations Delaware and Ithaca are small, although these stations are close to the zones “A” and “D”. The auroras are seen mainly northward from the observatories, as it is usually expected at mid-latitudes of the Northern Hemisphere, i.e., in the direction toward the auroral zone. The Fritz-Peak station is situated between zones “A” and “D”, which suggests observations of auroras both northward and southward. But for the period from August 1st to December 1st, 1957, there was only one case of observations in southward direction. The station Pulman is close to zone “A” in the western part of the continent. The number of auroras in the zenith was small and they were recorded mainly in northward direction. At the station Meanook, which is north of the zones “A” and “D”, one would expect by far more aurora toward south. But they appeared more often northward, toward the aurora zone.

#	Station	Coordinates			Zenith %	Number	
		$\phi$ , N	$\lambda$ , W	$\Phi'$ , N		N	S
1	Fritz-Peak	39°52'	105°31'	48.7°	2.2	82	1
2	Delaware	40°30'	83°	51.6°	3.6	152	26
3	Ithaca	42°27'	76°31'	53.8°	5.2	275	90
4	Pulman	46°43'	117°10'	53.5°	11.0	236	94
5	Meanook	54°36'	113°20'	61.8°	90.0	888	506

**Table 1.** Auroral observatories during the IGY with their coordinates (geographic latitude  $\phi$  and longitude  $\lambda$  as well as the corrected geomagnetic latitude  $\Phi'$ ; appearance of auroras in the zenith in per cent of the total and the number of observations northward (N) and southward (S) of the station.

3.9 The observations of auroras at the mid-latitude stations at the American continent, situated in the region of corpuscular precipitation that are formed by the mid-latitude parts of zones “A” and “D”, show the incorrectness of the planetary

precipitation scheme, which had been proposed by Nikolsky (1960). Along these zones, which stretch into mid-latitudes, zenith auroras are practically missing. Consequently corpuscular precipitations, which would lead to discrete auroral forms, are non-existent there. The existence of corpuscular precipitation regions, which extent into mid-latitudes or even to the equator during evening and nighttime hours, that would lead to the appearance of auroras at these latitudes, belongs rather to the genre of scientific fiction than to scientific results.

Referring to some morphological characteristics of magnetic disturbances at mid- and subauroral latitudes, Hope (1961) suggests, that they may be explained as disturbances transported from high to low latitudes by the ionospheric current system, probably identical with the  $S_D$  circulation. In addition we note that one cannot preclude a certain contribution to the disturbances at these latitudes originating from the magnetic fields of the magnetospheric currents systems and from the FACs between ionosphere and magnetosphere.

3.10 Mayaud (1956) studied the magnetic agitation in the polar region by using three-hourly amplitudes, obtained from the K-indices of 49 magnetic observatories at the Northern and Southern Hemispheres with  $|\Phi'| > 50^\circ$ . He separated nighttime and daytime types of agitation, which corresponds to the nighttime (N) and morning (M) maxima of activity according to the terminology of Nikolsky. Nighttime agitation is characteristic for magnetically disturbed days and maximizes at latitudes of the auroral zone (magnetic inclination of  $I \sim 77^\circ$ ). The time moment of reaching the maximum agitation in the diurnal variation at the auroral latitudes lagged behind those at neighbouring (northward and southward) latitudes. The daytime agitation is most characteristic for the near-polar region with  $I \sim 85^\circ$ , whose maximum is observed at local magnetic midday and shifted to  $\sim 06$  MLT at  $I \sim 81^\circ$ . The daytime agitation has maximum values in summer, minimum values in winter, and stays at a comparatively high level during magnetically quiet days. Daily averaged agitation values showed in the latitudinal dependence both for individual seasons and for the full year on average, that the 3-hourly amplitudes have one maximum at  $\Phi' \sim 65^\circ$ , but there is no disturbance enhancement in the near-polar region, which should be expected in case of a second, high-latitude maximum of the agitation.

3.11 Mansurov and Mishin (1960) investigated the Sa by using data from high-latitude stations in the Northern (19) and Southern (11) Hemisphere. Again the 3-hourly K-index was employed as measure of agitation. It was assumed that the Sa is controlled by local time and UT. That part, which depends on local time, is described as:  $S_0(t) = S_0 + K_1 \cos(t - \alpha_1) + \dots$ . They determined the amplitudes and phases of the first harmonics and modelled the dependence of the amplitude from geomagnetic latitudes for the winter and the summer season. During the winter, there exists only one maximum at  $\Phi \sim 67^\circ$ , but during the summer season there are two maxima at  $\Phi \sim 66^\circ$  and  $\Phi \sim 77.5^\circ$  in the latitudinal variation with a deep minimum at  $\Phi \sim 73^\circ$  in between. These

maxima are interpreted as zones of enhanced magnetic activity (agitation): the zone of maximal disturbances at  $\Phi \sim 66^\circ$  is thought to be coinciding with the main auroral zone and that at  $\Phi \sim 77.5^\circ$  coinciding with the second, high-latitude zone or region "B" according to Nikolsky (1960a). Such an interpretation of the latitudinal amplitude distribution of the first harmonic, that was made by Mansurov and Mishin (1960), differs from the general view on the zones of maximal magnetic agitation. The latter is usually characterized by the largest daily averaged agitation value, but not by the amplitude variation value in the course of the day. Further, the amplitude values of the first harmonic  $K_1$  is determined not only from the activity level, but also from the characteristic Sa value. The minimum of  $K_1$  at  $\Phi \sim 73^\circ$  might be caused by two Sa maxima at this latitude in different local times. The  $K_1$  values appear to be minimal during sufficiently strong daily averaged disturbance levels.

3.12 Beside of those studies, which employ statistical methods to derive regularities of magnetic disturbances, a number of scientists investigated the morphology of magnetic storms by comparing the magnetograms of various high-latitude observatories. Such a method was used in the studies of Birkeland (1913). The possibilities for applying this kind of methods extended greatly after the IGY. The data of a planetary-scale network of stations, collected in the World Data Centers, give a comprehensive perception of the global magnetic disturbances at all latitudes and longitudes. Results obtained by this kind of methods were presented, e.g., by Bobrov (1960).

3.13 Whitham and Loomer (1956) addressed in their investigations the question of the existence and position of a second zone of enhanced magnetic activity in the Canadian sector of the Arctic. The magnetic observatory Resolute Bay ( $\Phi' \sim 83^\circ$ ) is situated, according to Alfvén (1955) and Nikolsky (1956), directly under the second zone, while the station Baker Lake  $\Phi' \sim 73.7^\circ$  sits between the first and the second zone of enhanced magnetic activity. The comparison of the magnetic data of these two stations for the years 1953-1954 showed an interconnection between their disturbance states, but no unambiguous evidence for the existence of the second zone of corpuscular precipitation that spans above Resolute Bay.

Whitham et al. (1960) analysed the latitudinal variation of the magnetic disturbances based on 16 magnetic stations in Canada with  $54^\circ < \Phi' < 86^\circ$  for winter, equinox, and summer periods of the IGY. They used the hourly amplitudes of horizontal components (H, X, or Y) as the index of magnetic activity and the levels of activity were determined for all data as well as separately for the disturbed and the quiet days. It was concluded, that there exists a maximum in the latitudinal distribution at  $\Phi' \sim 67^\circ$  for all seasons and for all activity levels, in which during disturbed days the level reaches  $\sim 200$  nT. Confirming the former results of Whitham and Loomer (1956), no anomaly effects were found at the station Resolute Bay, which could indicate a second zone of

enhanced magnetic activity in the proximity of the station. Some activity enhancements at the station Alert ( $\Phi' \sim 85.7^\circ$ ) close to the geomagnetic pole were assumed to be due to a limited localized region of enhanced activity.

3.14 Some progress in the analysis of regularities in the spatial-temporal distribution of the magnetic activity at high latitudes came along with the research efforts of Burdo (1960). Observational material of 30 locations were used, unfortunately non-uniform in interval length, times of observation and the activity index used. He devoted particular attention in the study of the Sa forms, because the absolute amplitude of the magnetic disturbance depends essentially from the season and the index used. Seasonal variations could not be deduced, since the observations at 16 (out of 30) locations were shorter than one month. The latitudinal dependence on the maximum entry times in Sa appears to be more regularly when using the corrected geomagnetic latitude  $\Phi'$ , which takes into account the position of the station with respect to the auroral zone. This means according to Burdo (1960), that the magnetic activity at any time of the day is controlled by processes in the auroral zone. The activity is most intense at corrected geomagnetic latitudes of  $64^\circ < \Phi' < 66^\circ$  between 01–03 MLT. This maximum splits up with increasing latitude and becomes effectively two maxima – one at morning and the other at nighttime. The distance between the two maxima increases with further shift toward the pole. A third (evening) maximum at  $64^\circ < \Phi' < 66^\circ$  comes in at 17–19 MLT. With increasing  $\Phi'$ , the morning and evening maxima convene more and more and converge finally into one at  $\Phi' \sim 78^\circ - 80^\circ$ , which is found at 10–12 MLT. In observatories with the same distance to the auroral zone, but at different longitudes, the maximum occurs approximately at one and the same MLT. This fact serves as proof that the universal time has practically no influence on the form of Sa.

Synchronous hourly values of the disturbance vector  $\Delta T_{hor}$  at the stations Fort Rae ( $\Phi \sim 69.7^\circ$ ) and Tromsø ( $\Phi \sim 67^\circ$ ) were compared for 15–16 UT, when these stations are under the intense current regions of the morning and evening vortices, respectively. It turned out that the disturbances at both stations appear at the same time, i.e., with the increase of the disturbance intensity at one station it also increased at the other. This disproves the conclusion of Nikolsky (1951) about the independence on disturbances during the morning and evening hours. The disturbances thus appear simultaneously at the morning and evening side of the Earth, comprising the whole high-latitude region with maximum intensities close to the magnetic spirals.

3.15 The regularities of magnetic disturbances at high latitudes were studied by Feldstein (1963a) using data of a global set of stations from the IGY period. Hourly Q-index values of magnetic activity were used, which allow the study of diurnal and latitudinal variations of the activity (Bartels and Fukushima, 1956). This index characterizes the amplitude variations of the horizontal geomagnetic field component for 15-min intervals and accounts further for the maximum

deviation of these elements from the quiet time level. The disturbance of one hour is estimated at most by four 15-min intervals. Observations from 27 stations were used, which cover the high-latitudes of the Northern Hemisphere between  $58.4^\circ < \Phi' < 88.1^\circ$ . The IGY observations allowed at the highest level the use of homogeneous material both for the interval length and time of the observations as well as with respect to the activity index. Diurnal and latitudinal variations of the agitation were analysed separately for magnetically disturbed and magnetically quiet days. The form of the diurnal variation depends on season and to a great extent on the geomagnetic latitude of the observation.

3.16 The Sa has one maximum in the near-polar region during the winter season converging to the midday MLT hours (at stations Thule,  $\Phi' = 86.2^\circ$ , Resolute Bay,  $\Phi' = 83.0^\circ$ , and Godhavn,  $\Phi' = 77.5^\circ$ ). At lower geomagnetic latitudes, this maximum shifts to the morning hours and in the Sa appears a second, evening maximum (stations Murchison Bay,  $\Phi' = 75.1^\circ$ , Tikhaya Bay,  $\Phi' = 74.7^\circ$ , Baker Lake,  $\Phi' = 73.7^\circ$ , Cape Cheluskin,  $\Phi' = 71.6^\circ$ , and Point Barrow,  $\Phi' = 69.4^\circ$ ). At even lower latitudes, these maxima are difficult to discriminate as they merge to one single maximum approaching midnight hours (stations Dixon Island,  $\Phi' = 68.0^\circ$ , Leirvogur,  $\Phi' = 66.8^\circ$ , Kiruna,  $\Phi' = 65.4^\circ$ , College,  $\Phi' = 64.7^\circ$ , Murmansk,  $\Phi' = 64.1^\circ$ , Sodankylä,  $\Phi' = 63.0^\circ$ , and Meanook  $\Phi' = 61.9^\circ$ ). The Sa forms are better controlled by the corrected geomagnetic latitude (Hultqvist, 1958; Gustafsson, 1970) than by geomagnetic latitude. The stations Julianehab ( $\Phi = 70.8^\circ$ ,  $\Phi' = 68.7^\circ$ ) and Leirvogur ( $\Phi = 70.2^\circ$ ,  $\Phi' = 66.8^\circ$ ), which are located at relatively high geomagnetic latitudes, have only one near-midnight Sa maximum, which is characteristic for the auroral zone, but the stations Point Barrow ( $\Phi = 68.3^\circ$ ,  $\Phi' = 69.4^\circ$ ) and Cape Chelyuskin ( $\Phi = 66.2^\circ$ ,  $\Phi' = 71.6^\circ$ ) at relatively low latitudes have clearly two maxima (nighttime and morning), which is characteristic for stations at latitudes adjoining the near-polar region. The latitudinal anomalies in the Sa forms disappear, when replacing the geomagnetic latitude  $\Phi$  with the corrected geomagnetic latitude  $\Phi'$ . When moving from the auroral zone toward higher latitudes, the morning disturbances shift to later hours, and the nighttime disturbances to earlier MLT hours. Drawn in polar coordinates  $\Phi'$  versus MLT, the maxima in Sa are ordered along segments of spirals. The change in local time for varying latitudes is stronger for the morning maximum than for the nighttime maximum. There are no longitudinal differences in the time of maximum appearance for the Sa. This is an evidence for the unimportance of the UT moment for the positions of maxima in Sa.

3.17 In the summer season, the Sa behaviour is subject to substantial changes. From the geomagnetic pole down to  $\Phi' \sim 70^\circ$ , Sa is characterised now by one maximum in the prenoon MLT hours. At lower latitudes, one observes two maxima of Sa: one in the post-midnight to early morning hours and one in the afternoon to evening MLT hours. The Sa maximum in the afternoon to evening hours turn up as the



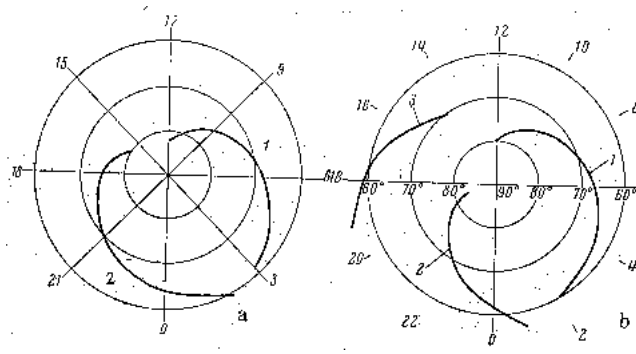


**Figure 5.** Dependencies of local geomagnetic time of Sa maximum occurrence on corrected geomagnetic latitude for magnetically disturbed days. a- winter, b summer 1 morning (M) maximum of agitation; 2 night (N) maximum of agitation; 3 evening (E) maximum of agitation (Feldstein, 1963a).

characteristic peculiarity of the summer season as it is missing in winter. Its appearance changes the form of Sa fundamentally during the transition from winter to summer at  $\Phi' \sim 60^\circ \div 70^\circ$ .

The analysis of Sa based on the Q-index of magnetic activity over all days of the winter and the summer season during the IGY proves the existence of morning, nighttime and evening agitation maxima at  $\Phi' > 60^\circ$ . Thereby each season has its own specified maxima: during summer in the morning and evening and during winter in the nighttime and morning hours. In the near-polar region one observes one single maximum during daytime hours.

3.18 Fig. 5 shows the moments of maxima in Sa in polar coordinates  $\Phi'$  versus MLT as observed during magnetically disturbed days of the winter (a) and the summer (b) season. The basic characteristics of Sa are kept during all days in the winter season (Fig. 5a). The diurnal activity variation has two maxima – during morning and nighttime hours. The morning maximum appears at later morning hours with increasing  $\Phi'$ , while the nighttime maximum appears earlier in the evening hours. The nighttime maximum, however, shifts faster toward earlier evening hours with increasing  $\Phi'$  than for observations, which comprise the full day, and at  $\Phi' \sim 80^\circ$  this difference in MLT attains four hours. The nighttime maximum appears at all stations up to the highest latitudes. The morning maximum clearly traces from the near-polar region to the latitudes of the auroral zone. The segments of the spiral, that correspond to the nighttime and morning Sa extremes, establish a shape, which reminds an oval, whose symmetry axis traverses the meridian 02–14 MLT.

During magnetically disturbed days of the summer season (Fig. 5b), there are three clearly established maxima of Sa activity at many stations. Three maxima appear crystal clear at the stations Arctica 2 ( $\Phi' = 77.5^\circ$ ), Tikhaya Bay ( $\Phi' = 74.7^\circ$ ), Cape Chelyuskin ( $\Phi' = 71.6^\circ$ ), Dixon Island ( $\Phi' = 68.0^\circ$ ), Murmansk ( $\Phi' = 64.1^\circ$ ), Sodankylä ( $\Phi' =$

63.0°), Cape Wellen ( $\Phi' = 62.5^\circ$ ), Meanook ( $\Phi' = 61.9^\circ$ ), and Lerwick ( $\Phi' = 59.4^\circ$ ). The three distinct maxima in Sa are obviously the characteristic peculiarity of the summer season during days of intense magnetic disturbances. Apart from the dependence on the magnetic activity level, during the winter season, as a rule, there exist not more than two maxima. The evening maximum does not appear related to the strong weakening of the disturbance intensity with  $\Delta H > 0$  during these hours. Such disturbances exist, but they do not appear as maximum in Sa at the background of the subsequent more intense disturbances with  $\Delta H < 0$ .

The intensity of the disturbances along the winter and summer spirals is different. During winter, the nighttime and morning disturbances maximize at latitudes of the auroral zone and become smaller toward higher latitudes. This decrease is very small till  $\Phi' \sim 75^\circ$ , but at higher latitudes the disturbance decreases sharply. During summer, the disturbances along the evening and morning spirals increases monotonically from mid-latitudes to the auroral zone and beyond that till  $\Phi' \sim 72^\circ$ , but for the morning maximum it remains at a high level until the near-polar region at  $\Phi' \sim 84^\circ$ .

3.19 What is the nature of the spiral distributions in the time moments of maximum values in Sa? There exist essentially two assumptions in the public literature: firstly, precipitation of corpuscular fluxes takes place along all spirals or at least along some of it (Nikolsky, 1956; Feldstein, 1963a) or, secondly, the spirals are the places of convergent current lines of the equivalent current system (Harang, 1946; Burdo, 1960). In the first case, the morning and nighttime spirals of the winter season should coincide with the position of auroras in the zenith, i.e., with the auroral oval, as the position of auroras points at the places of precipitating electrons with auroral energy into the upper atmospheric layers. The magnetic disturbance can be the result of processes, which take place far from the location of their records.

In Fig. 6 (from Akasofu, 1968) shows the M, N, and E spirals, obtained by Feldstein (1963a), together with the auroral oval according to Feldstein (1963b) in polar coordinates  $\Phi'$  versus MLT. This compilation shows, that during magnetically disturbed days the nighttime spiral N and during morning hours the M spiral are situated within the auroral oval, i.e., within the region of precipitating electrons with auroral energy. The N and M spirals, obtained from observations of the magnetic disturbances, are therefore positioned within the auroral oval of precipitating electrons. The evening spiral E adjoins to the equatorial side of the auroral oval. This is the region of the eastward electrojet and of precipitating protons with auroral energies and soft electrons (Starkov and Feldstein, 1970).

**4 Spirals in the distributions of auroras**

4.1 The daily variation of the occurrence frequency of visible auroras is an important aspect of the auroral activity. The

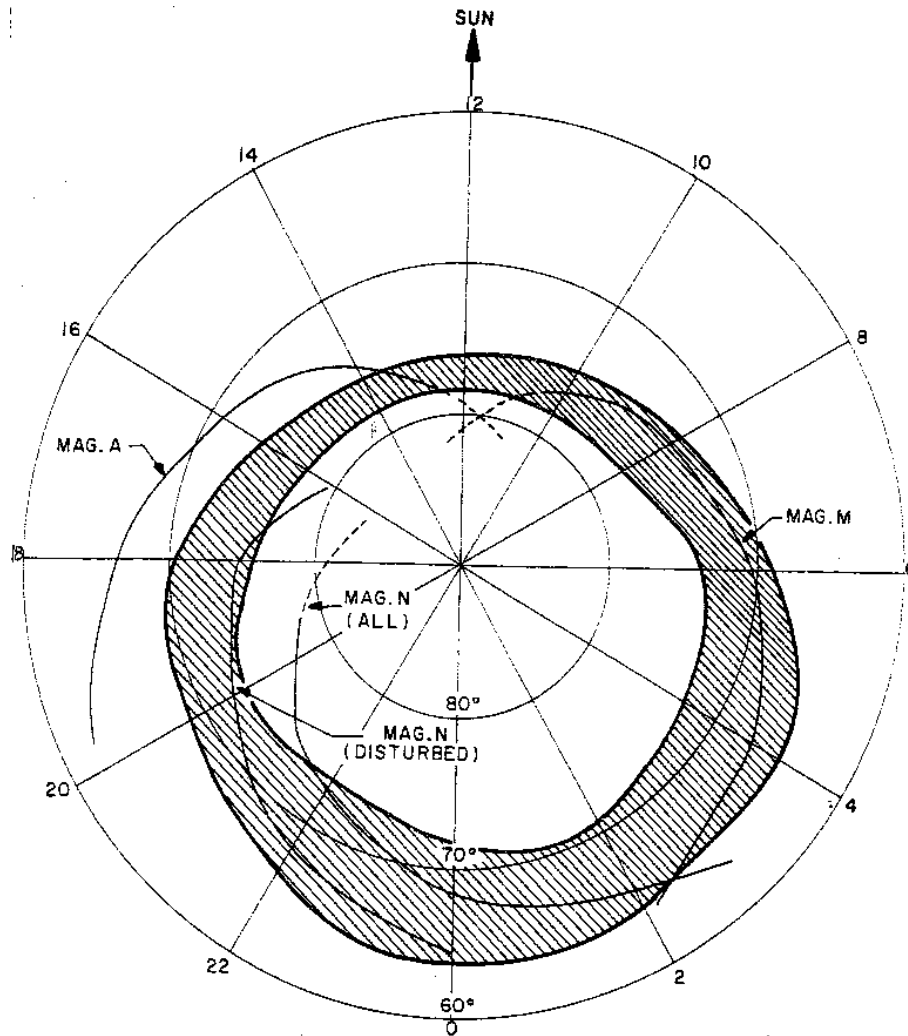


**Figure 6.** The M, N and E spirals determined by Feldstein (1963a) and the auroral oval by Feldstein (1963b) in dipole latitude and time coordinates (from Akasofu, 1968, Fig. 9).

1371 simplicity of its determination and the informative value of 1388  
 1372 this parameter for comparisons of the auroras with other geo-1389  
 1373 physical phenomena of the electromagnetic complex stimu-1390  
 1374 lated the appearance of a multitude of publications in this 1391  
 1375 field of research. Below we consider only a few of them, 1392  
 1376 which generalize the observations and give general impres-1393  
 1377 sions about acting physical regularities. 1394

1378 4.2 There is a tendency, that intense active discrete auroral 1395  
 1379 forms appear most often  $\sim 1$  hour prior to magnetic midnight 1396  
 1380 at latitudes of the auroral zone, as it was described by Ve-1397  
 1381 gard (1912) according to the materials of the First Interna-1398  
 1382 tional Polar Year (1882–1883). Additional to the nighttime 1399  
 1383 maximum, some high-latitude stations indicated a secondary 1400  
 1384 morning maximum (Tromholt, 1882; Isaev, 1940; Pushkov 1401  
 1385 et al., 1937). The accurate visual observations of auroras 1402  
 1386 performed by Tromholt at the station Godthab ( $\Phi' \sim 73.3^\circ$ ) 1403  
 1387 in Greenland attracted particular attention. The diurnal vari-1404

ation of the aurora occurrence frequency is characterized by  
 two maxima, one during late evening, the other during morning  
 hours, and a minimum shortly after midnight. The morning  
 maximum at 05–07 MLT was afterwards interpreted as  
 evidence for the existence of a second auroral zone in the  
 polar cap, where the occurrence frequency of auroras and of  
 intense magnetic disturbances maximizes (Nikolsky, 1960b).  
 The maximum during morning hours appears clearly in the  
 daily variations of visual data sets at the stations Kinga Fjord  
 ( $\Phi' \sim 77.8^\circ$ ) in Canada (Neumayer and Børgen, 1886) and  
 Tikhaya Bay ( $\Phi' \sim 74.7^\circ$ ) at Franz Joseph Land (Pushkov  
 et al., 1937; Isaev and Pushkov, 1958). This maximum is  
 absent in the records of some other stations. Analysing a  
 large amount of observational data, Hulburt (1931) comes to  
 the conclusion that the probability of the occurrence of a sec-  
 ondary morning maximum is as high as its absence.

Full-day visual aurora observations at Greenland are not

possible even during winter season, because of the daylight period from  $\sim 07$ – $17$  local time. This complicates the determination of the morning maximum and the frequency of its occurrence. Observations by Carlheim-Gyllenskiöld (1887) at the station Cap Thordsen, Spitzbergen ( $\Phi' \sim 74.3^\circ$ ), where practically a full-day monitoring is possible, confirmed the existence of two maxima - one in the morning and the other during pre-midnight hours MLT.

4.3 Based on hourly observations of the years 1954–1955 from 50 polar stations at geomagnetic latitudes  $57^\circ < \Phi < 80^\circ$ , Feldstein (1958) concluded: 1) the nighttime maximum attains maximal values at auroral zone latitudes ( $\Phi \sim 65^\circ$ ); 2) the shape of diurnal variations changes gradually with increasing latitude, and there appears a second maximum in the morning hours at ( $\Phi > 69^\circ$ ) with a smaller intensity of the absolute value than the nighttime one. In the near-polar region, the diurnal variation is sparsely developed and discrete forms appear likewise rarely both during nighttime and morning hours.

Lassen (1959a,b, 1961) investigated the diurnal variation of auroral occurrences at 5 Greenland stations for the years 1948–1950. It was concluded that the different types of diurnal distribution can be arranged according to the following scheme: 1) at latitudes of the main auroral zone, there is one maximum of auroral occurrence around midnight; 2) at latitudes from the main to the inner zone of auroras ( $8^\circ - 10^\circ$  poleward from the main zone), there appears a second, smaller morning maximum; 3) within the inner auroral zone, one observes clearly two maxima - one around midnight and the other at  $\sim 06$  MLT; 4) within the polar cap, the morning maximum dominates about the nighttime one. Subsequently Lassen (1963) analyzed the results of visual observations at many high-latitude stations for the interval of the  $I^{\text{st}}$  IPY (1882/83) and up to the begin of the IGY with respect to the daily variation of the frequency of auroral occurrences and obtained the following results: 1) stations in the latitudinal range  $64^\circ < \Phi < 69^\circ$  show a maximum near midnight; 2) between  $70^\circ < \Phi < 76^\circ$  an evening and a morning maximum of equal size are observed; 3) north of  $\Phi \sim 77^\circ \div 78^\circ$ , the morning maximum is dominating, it occurs late in the morning. Lassen (1963) could not find a regular displacement of the evening and morning maxima.

4.4 Visual observations in the above-mentioned investigations considered auroral forms that are visible over the entire sky. Assuming an elevation of 100 km for the lower borders of the auroras, such observations comprise  $\sim 17^\circ$  of latitude, from the northern to the southern horizon. Consequently, only a limited latitudinal discrimination was possible. By determining the geomagnetic times of the maximum occurrence probability for overhead auroras in  $1^\circ$  wide latitudinal ranges, Malville (1959) demonstrated at the stations Ellsworth ( $\Phi \sim 67^\circ$ ) and South Pole ( $\Phi \sim 77^\circ$ ), Antarctica, that the maximum time occurs systematically earlier in the evening as the pole is approached from the auroral zone. This dependence in polar coordinates  $\Phi$  versus MLT

arises as a part of the spiral in the range  $64^\circ < \Phi < 71^\circ$  in the evening sector. The publication of Malville (1959) is the first one, where the existence of a spiral regularity in the spatial-temporal distributions of aurorae is mentioned. Later it was extended both in latitudinal range and by including the distribution of the morning spiral.

4.5 During the IGY, a network of all-sky cameras operated at high latitudes, which produced photos of the sky in 1-min cadence with exposure times of 20 sec or 5 sec. The results of the perusal of the all-sky films were recorded in special tables - the so-called ascaplots, which allowed to localize the aurora on the sky, to exclude intervals of illumination times and of bad meteorological conditions. The ascaplots were assembled according to the instructions of Stoffregen (1959). The full sky was divided along the geomagnetic meridian into three zones: zenith (from  $30^\circ$  elevation north to  $30^\circ$  elevation above the south horizon), North (from  $10^\circ$  to  $30^\circ$  elevation above the north horizon), south (from  $10^\circ$  to  $30^\circ$  elevation above the south horizon). The extent of each stripe amounts to  $\sim 3^\circ$  of geomagnetic latitude. The report about the ascaplots of a global network of stations is given in Annals (1962).

4.6 Feldstein (1960) determined the diurnal variation of auroral occurrence frequency in the zenith for 24 stations of the Northern Hemisphere in the latitude range  $55^\circ < \Phi' < 85^\circ$ . Fig. 7 shows the characteristic shapes of the diurnal variation for various latitudes. In the auroral zone and equatorward of it clearly appears a maximum. It occurs at  $\sim 03$  MLT in Verkhojansk ( $\Phi' = 56.6^\circ$ ) and around midnight MLT for  $\Phi' \sim 65^\circ \div 66^\circ$  (Murmansk,  $\Phi' = 64.1^\circ$  and Wrangel Island,  $\Phi' = 64.7^\circ$ ). At higher latitudes between  $67^\circ < \Phi' < 78^\circ$ , there exist two maxima - one in the evening hours, the other in the morning (Arctica I at  $\Phi' \sim 72^\circ$  and Piramida, Spitzbergen at  $\Phi' \sim 77^\circ$ ). With increasing latitude, the morning maximum occurs later in the morning and the evening maximum occurs earlier. Already at  $\Phi' \sim 80^\circ$ , the auroras don't emerge at midnight as at auroral latitudes, but around midday. In the polar cap (Arctica II at  $\Phi' \sim 82^\circ$ , the auroras are rare, but if so, they appear mainly during daytime hours. The maximum around midnight at  $\Phi' \sim 73^\circ \div 75^\circ$  appears in visual observations of the full sky during the  $I^{\text{st}}$  IPY at Greenland and Spitzbergen as intense auroras with a southern azimuth at latitudes of the nighttime auroral zone.

The appearance times of the “nighttime” and “morning” maxima in  $\Phi'$ –MLT coordinates are distributed along two segment of straight lines. Transferring this relationship into polar coordinates (Fig. 8), then it results in a pattern, which reminds of an oval with minimum distance to the geomagnetic pole on dayside hours and maximum distance at night. The oval consists of two spirals with opposite sense. Fig. 8 represents the first full display of spiral regularities in the auroras of the Northern Hemisphere. A similar double spiral distribution for the Southern Hemisphere was obtained by Feldstein and Solomatina (1961). They are considered as the starting point for introducing the term “auroral oval” in

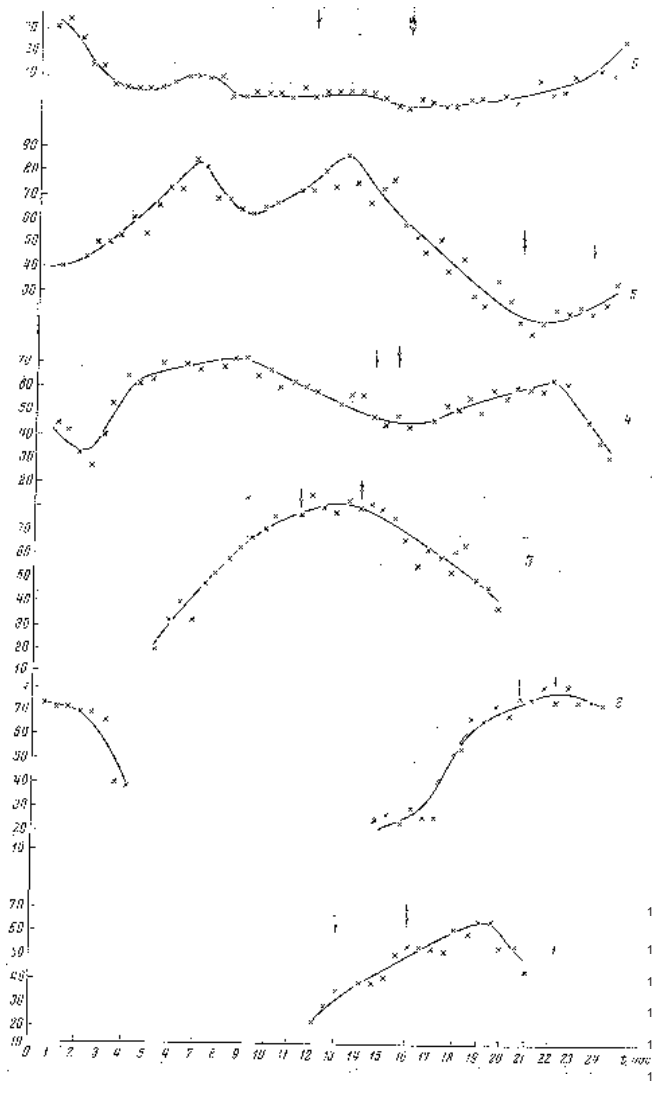


**Figure 7.** Diurnal variations of auroras appearance in zenith (Universal Time). 1 – Verkhoyansk; 2 – Murmansk; 3 – Wrangel Island, 4 – Arctic I (North Pole 6); 5 – Piramida (Spitzbergen); 6 – Arctic II (North Pole 7). Figures along the axis of ordinates signify the frequency of appearance of auroras at zenith (in percent). The arrow depicts local midnight, double arrow depicts local geomagnetic midnight (Feldstein, 1960).

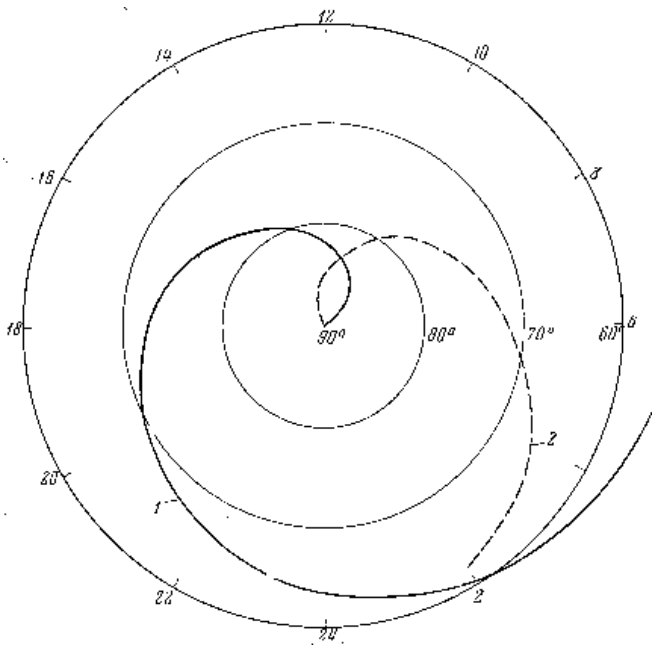


**Figure 8.** Dependence of occurrence times of MLT “night” and “morning” maxima in diurnal changes of probability of auroras appearance in zenith on geomagnetic latitude in polar coordinates (Feldstein, 1960). 1 – night maximum; 2 – morning maximum.

1515 solar-terrestrial physics, signifying the region, where ener-1542  
 1516 getic charged particles penetrate into the upper atmosphere.1543  
 1517 On the one hand the auroral oval is the region of the most1544  
 1518 frequent appearance of auroral forms in the zenith at a given1545  
 1519 geomagnetic latitude, but it signifies also the actual zone of1546  
 1520 auroral lights for the given moment in time. The oval is1547  
 1521 asymmetric with respect to the geomagnetic pole due to the1548  
 1522 deformation of the geomagnetic field by the solar wind. The1549  
 1523 discussions about the conception of the auroral oval contin-1550  
 1524 ued in the science community till the 70-ies of the past cen-1551  
 1525 tury as long as it didn't find its affirmation in the “Sputnik-1552

era” of active space exploration.

4.7 Lassen (1963) used aurora observations at four Greenland stations during the IGY to determine the diurnal variation of frequencies of occurrence in the zenith as well as northward and southward of the zenith. At the stations Godhavn ( $\Phi' = 77.5^\circ$ ), Kap Tobin ( $\Phi' = 72.7^\circ$ ) and Julianehab ( $\Phi' = 68.7^\circ$ ), auroral observations were not possible during 10 daytime hours because of the daylight. A continuous data set was achieved by the use of ascaplots from nine additional high-latitude stations in the Arctic and Antarctic. Four of them allowed auroral observations throughout the whole day. The moments of maxima in the diurnal variation are allocated close to two segments of straight lines. In polar coordinates the maxima rearrange along two spirals of opposite sense. These results coincide with the similar double spiral distribution shown by Feldstein (1960). Such a coincidence of the results of two independent investigations can be expected, considering the accordance in the selected data sets.

4.8 Magnetic disturbances and auroras constitute different aspects of the same electromagnetic complex of phenomena that take place at high altitudes. The magnetic variations, on the one hand, which are recorded at the Earth's surface, represent the integral effect of the corpuscular fluxes and of the current systems in the ionosphere, covering a considerable part of Earth, but the positioning of the auroras points directly to the location of precipitating corpuscular fluxes, that cause the magnetic disturbance.

The discussion of the interrelationship between the auro-  
 ras of different types and the plasma domains in the mag-  
 netosphere and their structure is beyond the scope of the  
 present review. Detailed considerations about the present  
 understanding of problems in auroral physics is contained  
 in the collective monograph on “Auroral Plasma Physics”  
 (Paschmann et al., 2002). Results about the projection of  
 the boundaries of various aurora types from ionospheric level  
 into the magnetosphere and the relation of their emissions  
 with the magnetospheric plasma domains are summed up by  
 Feldstein et al. (1994) and Galperin and Feldstein (1996).

## 5 Interpretations of the spiral regularities in mag- netic field variations and auroras

### 5.1 Magnetic spirals, their number and correlation with the ionospheric current system

The number of spirals appeared to be disputed, based on the  
 analysis of  $S_D$  variations of the geomagnetic field as dis-  
 cussed in the previous sections; according to Meek there are  
 two (M and E spirals), while according to Harang–Burdo–  
 Feldstein (“H.–B.–F.”) we have to deal with three of them  
 (M, N, and E spirals). Referred to Meek (1955), there could  
 be only two spirals, namely one that represents the max-  
 imimum decrease of the horizontal component ( $\Delta H < 0$ , M  
 spiral) or the other that represents the maximum increase  
 ( $\Delta H > 0$ , E spiral). A third spiral was not identified, as along  
 it also applies  $\Delta H < 0$ , but with a smaller amplitude than in  
 the deepest minimum. According to H.–B.–F., the spirals  
 match both extremal values in  $\Delta H < 0$  and a sign change in  
 $\Delta Z$ . The number of extremal values in the diurnal variation  
 of  $\Delta H$  changes in dependence on magnetic latitude from one  
 to three (the M, N, and E spirals). Three characteristic peaks  
 were also found in the diurnal variation of the Sa activity  
 (Chapman and Bartels, 1940; Nikolsky, 1951, 1956; Burdo,  
 1960; Feldstein, 1963a). Also Akasofu (2002) distinguishes  
 three spirals M, N, and E.

The magnetic spirals specify regions, where concentrated  
 isolines of the ionospheric equivalent current system  $S_D$  de-  
 scribe the magnetic field variations at high-latitudes. Two  
 spirals form the current oval: for Meek (1955) it consists of  
 the westward (M spiral) and eastward directed currents (E  
 spiral), while for H.–B.–F. only of westward directed (M and  
 N spirals). The current direction in the spirals is not unam-  
 biguously related to the direction of its winding: in the M  
 and N spirals with westward currents, the winding is in dif-  
 ferent directions; in the N and E spirals, which turn in one  
 and the same direction, the direction of the current is op-  
 posite to each other. The winding of the spiral is also not  
 determined by the sign of the charged particles that precipi-  
 tate into the upper atmosphere. Particles of the same sign are  
 precipitating along the M and N spirals (electrons of auroral  
 energy, that are forming the oval), but the winding direction  
 of these spirals differs.

### 5.2 Discontinuity in the ionospheric current of the auroral belt

5.2.1 The equivalent current system, which characterizes the  
 intensity and spatial distribution of geomagnetic disturbances  
 at high latitudes, was introduced by Chapman (1935). It  
 was a major paradigm for a few decades. Its characteris-  
 tic peculiarity consists in two concentrated current flows in  
 the auroral zone, which were named by Chapman as electro-  
 jets: the eastward electrojet (EE) appears in the evening sec-  
 tor and the westward electrojet (WE) on the morning side.  
 Between these electrojets exist discontinuities during a few  
 hours around midnight and midday.

5.2.2 Harang (1946, 1951) confirmed with his investiga-  
 tions, that the electrojets are located within the auroral zone  
 at  $\Phi \sim 67^\circ$  from evening to morning hours. This was to a  
 great extent due to the paradigm (ruling at that time) about  
 the positioning of a particle precipitation region at these lati-  
 tudes. The Harang study presented no drastic revision of the  
 conceptions regarding the structure of the high-latitude cur-  
 rent system. As before, the electrojets were associated with  
 the auroral zone. According to Harang a discontinuity be-  
 tween the WE and EE is located at latitudes of the aurora  
 zone but not along the auroral oval (yet unidentified at that  
 time). The morphology of the night time discontinuity be-  
 tween the electrojets was shown in detail in Harang (1946,  
 Fig. 2). It does not come to an agreement with his statement  
 about the discontinuity in the localisation at aurora zone lati-  
 tudes. The electrojets overlap each other in the dusk sector  
 (in the sense that the EE and WE coexist at the same local  
 time but at different latitudes) and the westward current is lo-  
 cated there poleward of the eastward. Between the electrojets  
 there exists no discontinuity, according to his data, but rather  
 a gap, whose latitude varies between evening and nighttime  
 hours. The westward electrojet is not delimited by the mid-  
 night meridian, but extends toward the evening sector, posi-  
 tioned at higher latitudes with respect to the eastward electro-  
 jet. Due to this, the electrojets don’t stay strictly within the  
 auroral zone at  $\Phi \sim 67^\circ$  from the evening to the morning side,  
 but comprise also slightly higher latitudes. For the western  
 electrojet during nighttime any discontinuity is absent; the jet  
 rather continues steadily in LT from morning hours over the  
 nighttime to evening hours.

5.2.3 According to Burdo (1960) the latitude of the dis-  
 continuity between the electrojets increases from  $\Phi' \sim 65^\circ$   
 at midnight to  $\Phi' \sim 75^\circ$  at  $\sim 20$  MLT. Those processes that lead  
 to the generation of currents, which are responsible for the  
 observed geomagnetic variations, are both for Harang and  
 Burdo the precipitation of corpuscular fluxes at auroral zone  
 latitudes (the existence of an auroral oval was not known at  
 the time of their publications). Currents at higher latitudes  
 start-up due to the dynamo effect. The existence of dynamo  
 electric fields is also necessary, as they are generated at iono-  
 spheric altitudes owing to the neutral wind motion within  
 these layers. The dynamo current system at ionospheric alti-

tudes is two-dimensional and controlled by processes in the upper atmosphere close to Earth.

5.2.4 The discovery of the auroral oval brought about a new stage for the interpretation of the discontinuity between the electrojets. This discovery led to a fundamental change in the conception of the planetary morphology concerning the electro-magnetic complex in the near-Earth space (Akasofu and Chapman, 1972). The active auroral forms and hence the most frequent and most intense corpuscular precipitations into the upper atmosphere are distributed along the auroral oval and not along the auroral zone. It was shown, that the westward electrojet runs along the auroral oval from the evening to the morning MLT hours (Feldstein, 1963b; Feldstein and Zaitzev, 1965b; Akasofu et al., 1965; Akasofu and Meng, 1967a,b,c; Starkov and Feldstein, 1970).

The location and configuration of the auroral oval is intimately connected with the asymmetric shape of the Earth's magnetosphere in the Sun-Earth direction (O'Brien, 1963; Frank et al., 1964; Feldstein, 1966), with the plasma structure of the magnetosphere (Vasyliunas, 1970; Frank, 1971; Winningham et al., 1975; Feldstein and Galperin, 1985), and in particular with the plasma sheet in the magnetospheric tail. The eastward electrojet runs in the evening sector at latitudes of diffuse luminosity, adjoining the auroral oval at the equatorial side. This luminosity is caused by the precipitation of low energy electrons from the inner magnetosphere with energies up to  $\sim 10$  eV, which are convected from the plasma sheet in the Earth's magnetotail (Nishida, 1966; Feldstein and Galperin, 1985), and by protons with energies of  $\sim 10$  keV, which are formed in the magnetosphere in the partial ring current of westward direction (Grafe et al., 1997; Liemohn et al., 2001). Its short-circuit by FACs through the ionosphere causes the appearance of the eastward electrojet in the ionosphere. This way the emergence of the auroral oval conception combined the existence of the gap between the eastward and westward electrojet with the magnetospheric plasma structure.

5.2.5 In the course of 30 years (from 1935 till 1965), both the morphology and the physical conception of the nighttime discontinuity in the equivalent ionospheric current system changed successively, Heppner (1972) proposed to call it the Harang discontinuity. This term has been consolidated since that time in the scientific literature as designation of the discontinuity between the electrojets. Note that the existence of the discontinuity was found by Harang in 1946 (see, e.g., Zou et al., 2009). Apparently, when discussing the discontinuity between the electrojets as a natural phenomenon, debated intensively for a long time, one has to give credit to various cutting-edge research efforts:

- Chapman–Harang (CH) – discontinuity at auroral zone latitudes during near midnight hours;
- Harang–Burdo (HB) – for increasing latitude of the discontinuity in the evening sector, it shifts from midnight to evening hours. The generation of electrojets

in the ionosphere and the discontinuity between them are caused by the precipitation of auroral particles and therefore the enhanced ionospheric conductivity at latitudes of the auroral oval as well as by the neutral wind system in the ionosphere. The dynamo action is responsible for the appearance of a 2-D current system at ionospheric heights;

- Feldstein–Akasofu (FA) – no discontinuity, but rather a gap between the eastward and westward electrojets. The morphology of the current gap is analogue to the current discontinuity of HB, but the physical reason for the gap appearance is different. In actuality, there occurs no discontinuity of the electrojet, because in the westward electrojet any discontinuity is missing. The electrojet does not break apart, but continues from nighttime to evening hours, shifting toward higher latitudes. Resulting from that, between the electrojets appears a gap. This gap reflects the boundary of large-scale plasma structures in the nightside magnetosphere. The westward electrojet along the auroral oval is connected with the central plasma sheet in the magnetospheric tail, while the eastward electrojet – with the Alfvén layer in the inner magnetosphere (Feldstein et al., 2006). The electrojets appear as elements of a 3-D current system, which extends throughout the Earth's ionosphere and magnetosphere (Lyatsky et al., 1974; Akasofu, 2004; Marghitu et al., 2009).

## 6 Current systems of polar magnetic disturbances

6.1 The description of geomagnetic field variations by means of equivalent currents at ionospheric level and later also in its 3-D extension within the Earth's magnetosphere, has a long history. The sequential progression of perceptions in this field of geophysics was accomplished by the contributions of such “titans” of science like Kristian Birkeland, Sydney Chapman, Hannes Alfvén, Takesi Nagata, and many other outstanding scientists. It is beyond the scope of this review to consider this history, we rather have to confine ourselves to a short demonstration of the present-day views about the spatial-temporal characteristics of the current system in the near-Earth space (Akasofu, 2002; Feldstein et al., 2006).

6.2. Modelling of equivalent ionospheric currents, based on magnetometer data on the Earth's surface, can be realized with different methods. The direction and intensity of the linear current can be found by rotating the horizontal magnetic disturbance vector clockwise by  $90^\circ$  (Kamide and Akasofu, 1974; Baumjohann et al., 1980). Based on data from 70 magnetic observatories, including six meridional chains of magnetometers, Kamide et al. (1982) obtained the spatial distribution of ionospheric current densities for four UT cross-sections during a substorm on 19 March 1978. An overview of various techniques used for simulations of the equivalent

currents from ground-based magnetometer data was given by Untiedt and Baumjohann (1993).

6.3. Kotikov et al. (1991) developed a practical inversion scheme to infer the fine structure of the auroral electrojet by utilizing a series of linear ionospheric currents (50 al- together) of different intensities located at 100 km altitude. The current distribution was adjusted to fit measurements on the Earth's surface. This numerical method for estimation of equivalent ionospheric currents, using magnetic field observations along meridian chains of ground-based vector magnetometers, allows not only for the determination of the latitudinal distribution of the ionospheric current intensity but also for the separation of the contributions to the observed geomagnetic variations of the fields from external (ionospheric and magnetospheric) and internal (induced by telluric currents) sources. Popov and Feldstein (1996) and Popov et al. (2001) suggested a refinement of the Kotikov method by approximating the auroral electrojets with a series of narrow current strips of finite width. The strips with currents of different intensities were distributed along a geomagnetic meridian at 115 km altitude over the range of latitudes covered by the ground magnetometer stations. Both the accuracy of the method and its spatial resolution were considered in detail by Popov et al. (2001).

6.4. Feldstein et al. (2006) applied the refined method of Popov and Feldstein (1996) to some substorms and a magnetic storm in order to obtain the location and distribution of eastward and westward electrojet intensities as a function of latitude. For that study were used data from three meridian magnetometer chains: the IMAGE chain along the 110° CG (corrected geomagnetic) longitude meridian; the GWC chain along the 40° CG longitude meridian; the CANOPUS chain along the 330° CG longitude meridian.

The observed magnetic field variations in the vertical (downward) and horizontal H (northward) components at any point "l" along the geomagnetic meridian at the Earth's surface due to a single current strip is given by

$$H_{ext}(l) = \frac{j_i}{2\pi} \left\{ \arctan \frac{x_i+d}{h} - \arctan \frac{x_i-d}{h} \right\} \quad (6)$$

$$Z_{ext}(l) = \frac{j_i}{4\pi} \ln \left\{ \frac{h^2 + (x_i+d)^2}{h^2 + (x_i-d)^2} \right\} \quad (7)$$

where  $j_i$  is the current density in the  $i^{th}$  strip,  $d$ ,  $h$ , and  $x_i$  are the half-width, the altitude, and the distance from the observation point to the ground projection of the centre of the  $i^{th}$  strip, respectively. Using these expressions for each of the magnetometers in the chain we obtain 2K equations to determine the current densities in N strips ( $N=100$ ). If  $N > 2K$ , the problem is underdetermined and the solution is not unique. In order to constrain the solution the regularization method developed by Tikhonov and Arsenin (1977) is used.

6.5. Latitudinal current density distributions for every chain with a 10-min cadence were the basis for the creation of equivalent ionospheric current patterns in the course of

the DP intervals. Such patterns are usually used for generalized representations of perturbed geomagnetic field vector distributions on the Earth's surface. Fig. 9a-e shows schematically various current system patterns, that were reported in the literature by different authors. They comprise the classical two-vortex current system (Chapman, 1935; Fukushima, 1953) (Fig. 9a), the single-vortex system with a WE along the auroral oval (AO) and closure currents through the polar cap and at mid-latitudes (Fig. 9b) reported by Feldstein (1963b) and Akasofu et al. (1965), and the two-vortex system with a WE within the boundaries of the AO and with an EE in the evening sector at  $\Phi \sim 65^\circ$  (Feldstein and Zaitzev, 1965b) (Fig. 9c). It was concluded that during substorms the WE extends to all longitudes along the AO and its intensity decreases from midnight to noon hours. The EE as a separate current system, rather than a return current from the WE, is located at  $\Phi \sim 65^\circ$  in the evening sector.

6.6. A modification of these patterns (Fig. 9d,e) for substorm and storm intervals was realised by Feldstein et al. (2006). The space-time distribution of currents and their structure at high latitudes during a polar magnetic substorm with an intensity of  $AL \sim -800$  nT is shown in Fig. 9d. The locations of the WE (red strip), EE (green strip) and PE (polar electrojet: dark blue strip) are shown.

6.7. The narrow strip ( $2^\circ$ - $3^\circ$  width in latitude) of the PE is located at the latitudes  $78^\circ < \Phi' < 80^\circ$  under quiet magnetic conditions. These are typical for the ionospheric projection of cusp latitudes around noon. At substorm maximum both PE and cusp shift towards  $\Phi \sim 73^\circ \div 75^\circ$  (Fig. 9d). Both intensity and direction of the PE are controlled by the IMF  $B_y$  component (eastward for  $B_y > 0$  or westward for  $B_y < 0$ ) [Feldstein, 1976 and references therein]. A number of pioneering investigations, devoted to PE and its connection with IMF, are quoted below. Svalgaard (1968) was the first who indicated the existence of two characteristic types of magnetic field variations in the polar regions. The disturbances occur simultaneously in the north and south polar caps and are controlled by the IMF sector polarity. The dependence on the magnetic field variations in the polar regions on the IMF sector polarity was independently obtained by Mansurov (1969). Friis-Christensen et al. (1972) and Sumaruk and Feldstein (1973) discovered independently and simultaneously, that those magnetic field variations are not controlled by the IMF sector polarity, but by the direction of the IMF azimuthal  $B_y$  component. Friis-Christensen and Wilhelm (1975) and Feldstein et al. (1975) used a regression method for extracting the  $B_y$ -controlled fraction of the high-latitude magnetic field variations and identified the corresponding equivalent DPC( $B_y$ ) current systems. The detailed description of this type of magnetic field variations and corresponding DPC( $B_y$ ) current systems can be found in the review (Feldstein, 1976, and references therein). The PE is a characteristic feature of DPC( $B_y$ ) current system. The PE intensity during the summer season for the IMF  $B_y \sim 6$  nT is  $\sim 1.8 \times 10^5$  A.

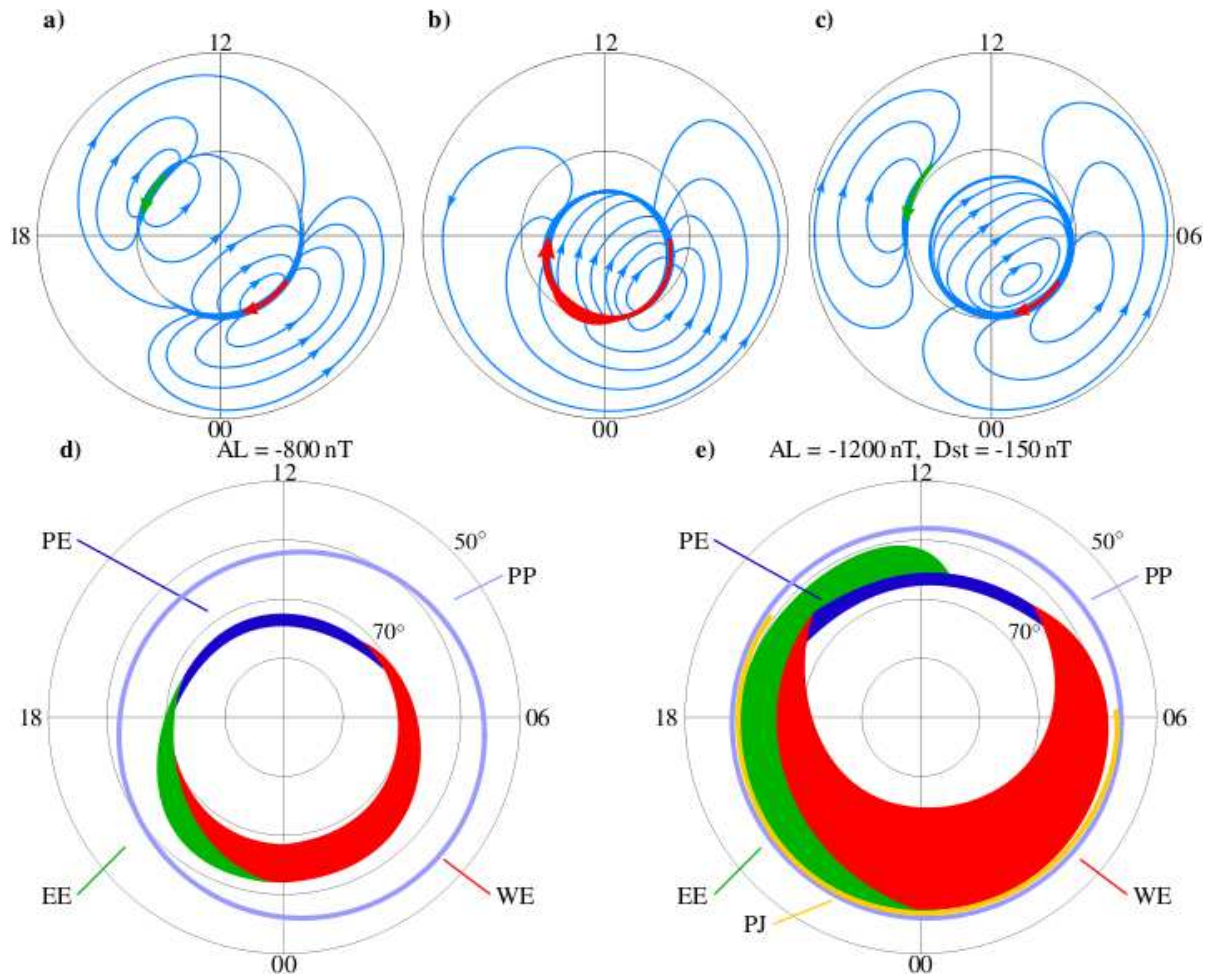


**Figure 9.** Schematic view of the electrojet’s space-time distribution at ionospheric altitudes: a) classical current system according to (Fukushima,1953); b) single-vortex system with westward electrojet along the auroral oval according to (Akasofu et al., 1965); c) double-vortex system with westward electrojet along the auroral oval and eastward electrojet in the evening sector at latitudes of the auroral zone according to (Feldstein and Zaitsev, 1965b); d) the magnetospheric substorm with  $AL \sim -800 \text{ nT}$ ; e) the magnetic storm main phase with  $AL \sim -1200 \text{ nT}$ ,  $Dst \sim -150 \text{ nT}$  (d and e by Feldstein et al., 2006).

1868 6.8. During substorm intervals the characteristics of the <sup>1883</sup>  
 1869 eastward/westward currents as far as their intensities and lo-<sup>1884</sup>  
 1870 cations are concerned, can be summarized as follows: <sup>1885</sup>

- 1871 – westward currents are most intense after midnight hours, <sup>1887</sup>  
 1872 at auroral latitudes of  $65^\circ < \Phi < 70^\circ$ , and are shifted <sup>1888</sup>  
 1873 to cusp latitudes ( $\Phi \sim 73^\circ$ ) in the morning and evening <sup>1889</sup>  
 1874 sectors. Its latitudinal width is  $\sim 6^\circ$  during midnight-<sup>1890</sup>  
 1875 dawn hours. As seen in Fig. 9d the WE does not cover <sup>1891</sup>  
 1876 all MLT hours (contrary to Figs. 9b,c) during the sub-<sup>1892</sup>  
 1877 storm, but is seen only within evening-night-morning <sup>1893</sup>  
 1878 hours. During pre-noon and late afternoon hours the <sup>1894</sup>  
 1879 WE adjoins the cusp, i.e., it is magnetically mapped to <sup>1895</sup>  
 1880 the magnetopause; <sup>1896</sup>
- 1881 – eastward currents in the evening sector start from cusp <sup>1897</sup>  
 1882 latitudes ( $\Phi \sim 73^\circ$ ) during the early afternoon MLT <sup>1897</sup>

hours, become most intense in the evening MLT, and reach auroral latitudes at nighttime hours. The EE comprises the evening sector from early evening to midnight hours and is located at lower latitudes when approaching midnight. During midnight the EE latitude is the same as that of the WE equatorward edge. Both the EE width and its intensity reach maximum values during dusk hours;

- eastward currents are located just equatorward of the westward currents for evening hours where currents in opposite directions overlap in latitude. During evening hours, when overlapping occurs, the maximum eastward current intensity is higher than the westward current intensity at the same local time;
- the EE shown in Fig. 9d is not a closure current for



the WE at higher latitudes, contrary to Fig. 9b, and is not located in the auroral zone ( $\Phi \sim 65^\circ$ ), contrary to Fig. 9c. During early evening hours the EE adjoins the ionospheric projection of the cusp (CU), i.e. the EE is magnetically mapped to the magnetopause during this MLT interval.

It is clear from Fig. 9d that the WE is located along M and N spiral segments, but it does not cover the MLT hours near midday. Such peculiarity in the WE structure is determined by the character of its connection with the central plasma sheet in the magnetospheric tail. The EE is located immediately equatorwards of the WE, along the E-spiral.

6.9. In Fig. 9d the location of the projection of the plasma-pause (PP) to ionospheric altitudes is indicated by the quasi-circle (blue). There is a latitudinal gap (of a few degrees) between the PP and EE that decreases when reaching night hours. During substorms this latitude gap is comparable to the EE width.

6.10. Fig. 9e shows the distribution of equivalent currents and their structure during the storm main phase with activity indices of  $AL \sim -1200 \text{ nT}$  and  $Dst = -150 \text{ nT}$ . The following characteristics of the electrojet dynamics are apparent:

- during evening hours both the EE and WE shift equatorward and the intensity of the electrojets increases;
- the eastward and westward current intensities in the evening sector imply that the EE cannot be the consequence of the WE closing through lower latitudes; it is likely that these electrojets are signatures of different geophysical phenomena;
- at the peak of the storm main phase the equatorward boundary of the CU (and hence the PE) shifts to  $65^\circ < \Phi' < 67^\circ$  and the width is  $2^\circ \div 3^\circ$ . During the late morning and early evening hours the westward currents adjoin the PE;
- at the main phase maximum the EE during near-noon hours adjoins the CU at  $\Phi' \sim 65^\circ$ , the WE is absent in the day-time sector;
- the WE asymmetry with regard to the noon-midnight meridian is valid for storm intervals (similarly to the substorm intervals). However, the asymmetry pattern changes essentially; in the night sector the WE poleward boundary is located at higher latitudes than the PE in the noon sector;
- the WE in the midnight and early morning sectors has a current density of  $\sim 1.6 \text{ kA/km}$ , and the integrated current is  $\sim 2 \div 3 \text{ MA}$ .

6.11. During the main storm phase the bursts of the ion drift velocity attain as much as  $\sim 4 \text{ km/s}$  at subauroral latitudes (outside of the plasmopause) in the region of the ionospheric trough. Galperin et al. (1974) was the first to report

strong poleward-directed electric fields driving fast plasma convection bursts at subauroral latitudes in the evening local time sector and called them polarization jets (PJ). The new name SAPS (Sub-Auroral Polarization Stream) is generally accepted nowadays for this phenomenon (Foster and Burke, 2002). In Fig. 9e the location of the bursts are indicated by a yellow line, the longitudinal prolongation of which is adapted from Foster and Vo (2002). Galperin (2002) proposed a model that explains the formation of PJ or SAPS during magnetic substorms and storms in the evening-to-nighttime sector of the discontinuity region between the auroral electrojets. A detailed consideration of the interrelation between auroral luminosity, FAC and PE during magnetic disturbances in the dayside sector was given by Sandholt et al. (2004).

6.12. To show the structure of magnetospheric plasma domains and the 3D current systems, a cross-section of the Earth's magnetosphere is displayed in Fig. 10. It is shown there with cuts in the midday-midnight meridional plane and in the equatorial plane, using ground-based observations of different auroral luminescence types and auroral precipitation (Galperin and Feldstein, 1991). The majority of plasma domains seen in the figure are directly related to large-scale current systems in the magnetosphere. Such FAC systems exist permanently in the magnetosphere (Maltsev and Ostapenko, 2004).

6.13. The 3D structure of currents in the near-Earth space is enclosed by the magnetopause. The currents screening the magnetic field of the inner magnetosphere from penetrating into the solar wind are located on the magnetopause. These eastward Chapman-Ferraro (CF) currents screen the dipole field. The magnetopause screening currents for the ring current (RC) fields are in the same direction, but their intensity is an order of magnitude weaker. The tail current (TC) in the central plasma sheet (CPS) is in the dawn-dusk direction. The closure of the TC is attributed to currents on the magnetopause which exist not only on the night side, as well established, but on the day side as well. In Fig. 10 the TC in the equatorial plane of the magnetosphere is indicated by two vectors. At midnight one of them is located in the innermost part of the current sheet, the other along its boundary. Their continuation on the magnetopause can be seen. However, the first remains in the tail and the second reaches the day side of the magnetopause where the directions of the CF and TC are opposite as seen in Fig. 10. Since CF currents are always more intense than TC closure currents the resulting current on the day side is always eastward.

6.14. The field aligned current flowing into and out of the ionosphere in the vicinity of the PE are located on the cusp surface. In Fig. 10 PE-FACs are indicated by two green lines (not vectors) along the magnetic field. The PE-FAC direction is not shown since it is controlled by the IMF  $B_y$  component: under  $B_y > 0$  ( $B_y < 0$ ) the current flows into (out of) the ionosphere along the cusp inner surface and out of (into) it along its outer surface. The ionospheric closure of the inflowing

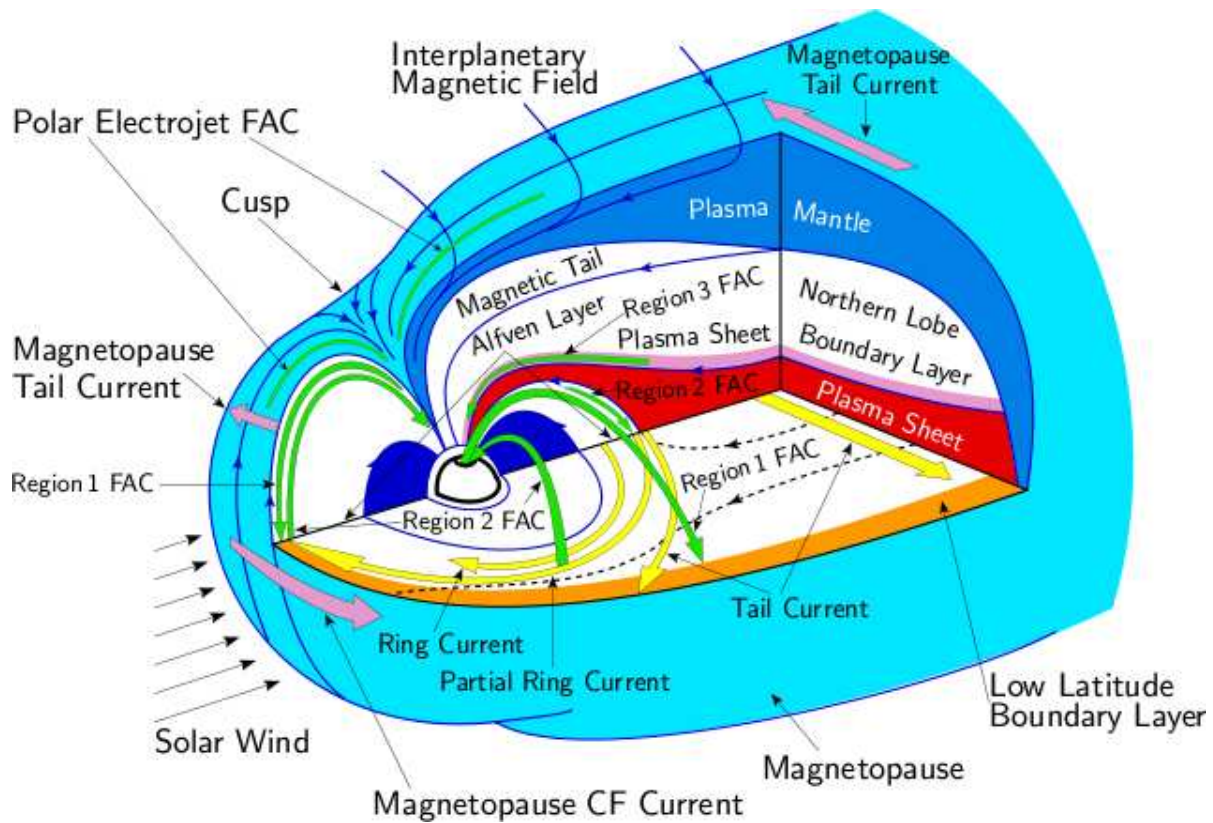


**Figure 10.** The 3-D system of electric currents in the magnetosphere during magnetic disturbances (Feldstein et al., 2006). Descriptions of the current system and the magnetospheric plasma structures are given in the text.

and outflowing PE-FAC is by Pedersen current. Its direction in the ionosphere is identical with the direction of the solar wind electric field component  $V \times B_y$ , i.e. under  $B_y > 0$  ( $B_y < 0$ ) the electric field in the cusp is poleward (equatorward) at ionospheric altitudes. In the cusp the Hall current in the form of the PE, spreading in the ionosphere (out of the cusp) is generated by this electric field. The PE is eastward (westward) under  $B_y > 0$  ( $B_y < 0$ ).

6.15. The Region 1 FAC in the dusk sector is usually believed to be mapped magnetically from the ionosphere to the low latitude boundary layer (LLBL), i.e., to the periphery of the magnetosphere, in the vicinity of its boundary with the solar wind. Such a pattern is valid for Region 1 FAC during day-time hours only and is shown by a current arrow, resting against the LLBL. During the dusk to pre-midnight hours where Region 1 FAC is located at AO latitudes, FACs inflow to the CPS, i.e., into the deep magnetosphere. In Fig. 10 the second current arrow of the Region 1 FAC crosses the equatorial cross-section of the magnetosphere in the dusk sector of the CPS behind the TC vector that depicts the current along the TC boundary.

6.16. The Region 2 FAC flows into the ionosphere from the Alfvén layer periphery, where the partial ring current (PRC) is located. In Fig. 10, the Region 2 FACs are indicated

by three vectors for day, dusk, and nighttime hours. It is generally believed, that the Region 2 FACs are located in the inner magnetosphere and part of a single current system with the EE and PRC. As seen in Fig. 10, the Region 2 FACs are flowing into the ionosphere during evening hours and are located in the magnetosphere at  $L \sim 4$ . In the early afternoon sector, where the EE adjoins the PE, the Region 2 FAC in the equatorial plane of the magnetosphere is near the LLBL.

6.17. The auroral electrojets present a continuation of the FACs at ionospheric altitudes. Eastward/westward electrojets are connected with magnetospheric plasma domains (the Alfvén layer / the CPS) via FACs. In known models of the EE, the Pedersen current in the ionosphere along with the Region 2 FACs constitute Boström’s Case I current system (Boström, 1964). At the same time, the Region 2 and Region 1 FACs in the evening sector constitute Boström’s Case 2 current system. The northward electric field between these FACs leads to Hall currents along the EE. Hence, the EE has a joining effect of Pedersen and Hall currents in the ionosphere.

6.18. As mentioned above, a characteristic morphological feature of auroral electrojets exists in the evening sector, namely in their overlapping. This is due to an additional Region 3 FAC current flowing into the ionosphere from the

PSBL during intense magnetic disturbances. A triple FAC structure arises. In addition to the Region 1 FAC and Region 2 FAC, the Region 3 FAC (flowing into the ionosphere) located on the poleward boundary of the auroral precipitation region appears. As a result, the necessary prerequisites for overlapping auroral electrojets are created. A southward electric field, favourable for the appearance of westward ionospheric Hall currents near the PC boundary, appears between the Region 3 FAC and Region 1 FAC. As a result a spatial overlapping of electrojets takes place. Also worth noting is that the WE represents the resultant effect of Pedersen and Hall currents in the ionosphere.

## 7 Conclusions

Spiral distributions (spirals) were used in the first stage of investigations for explaining the positioning of charged particle fluxes, precipitating into the upper atmosphere. Later they found their place (and became an intrinsic part) in global spatial-temporal patterns of some high-latitude geophysical phenomena. Below we list the basic peculiarities, that characterize the spirals in magnetic disturbances and auroras.

With respect to geomagnetic disturbances:

1. There are three types of spirals at high latitudes independent of seasons, named as M (morning), N (nighttime), and E (evening) spirals. The first two (M and N) appear distinctly and visibly during all seasons; the third one (E) is characteristic for the summer season.
2. Maximum intensities of ionospheric currents are observed along these spirals - the westward electrojet along the M- and N-spirals, and the eastward electrojet along the E-spiral.
3. Spirals with westward ionospheric currents are situated along the auroral oval from the late morning, over the nighttime till the early evening hours.
4. The windings of the spirals in clockwise or anticlockwise direction are not determined by the current flow direction in the spiral nor by the sign of the charged particles, which precipitate into the upper atmosphere.

With respect to auroras:

5. The visual observation of auroras is confined at high latitudes primarily to the winter season for the most part of the day. Only M- and N-spirals are identified, which constitute the auroral oval. Most often there appear discrete auroral forms in the zenith along the auroral oval.
6. Discrete auroral forms along the M- and N-spirals are due to precipitating electrons with energies up to a few  $keV$ . In the vicinity of the E-spiral, one observes diffuse auroras, which are due both to low-energy electrons and protons with energies of 10  $keV$  and higher.

7. The spiral distributions are not related to the dynamo action at ionospheric heights. The existence of the spirals and their distribution is determined by large-scale structures of plasma domains at the night side of Earth. The M- and N-spirals are connected with the inner (near-Earth) part of the central plasma sheet in the magnetospheric tail. The E-spiral relates, however, to the region between the central plasma sheet and the plasmopause, where the partial ring current is situated in the evening sector and where the low-energy plasma drifts in sunward direction out of the central plasma sheet.
8. There is no discontinuity between the westward and eastward auroral electrojet at a fixed latitude around midnight, but rather a gap, the latitude of which increases smoothly from nighttime to evening hours.

**Acknowledgements.** The authors express their gratitude to V. G. Vorobjev, and V. L. Zverev for reading the manuscript and for their critical comments. Support was obtained by RFBR grant No. 11-050036 to IZMIRAN. Work at GFZ Potsdam (M.F.) was supported by Deutsche Forschungsgemeinschaft (DFG).

## References

- Agy, V.: Spiral patterns in geophysics, *J. Atmos. Terr. Phys.*, 19, 136–140, 1960.
- Akasofu, S.-I.: Polar and magnetospheric substorms, D. Reidel, Dordrecht, The Netherlands, 316p., 1968.
- Akasofu, S.-I.: Exploring the secrets of the aurora, Kluwer Academic Publishers, Dordrecht/Boston/London, 235p., 2002.
- Akasofu, S.-I.: Several 'controversial' issues on substorms, *Space Sci. Rev.*, 113, 1–40, 2004.
- Akasofu, S.-I. and Chapman, S.: *Solar-Terrestrial Physics*, Oxford University Press, London, 1972.
- Akasofu, S.-I. and Meng, C.-I.: Intense negative bays inside the auroral zone-I. The evening sector, *J. Atmos. Terr. Phys.*, 29, 965–970, 1967a.
- Akasofu, S.-I. and Meng, C.-I.: Auroral activity in the evening sector, *J. Atmos. Terr. Phys.*, 29, 1015–1019, 1967b.
- Akasofu, S.-I. and Meng, C.-I.: Polar magnetic substorm in the evening sector, *J. Atmos. Terr. Phys.*, 29, 1027–1035, 1967c.
- Akasofu, S.-I., Chapman, S., and Meng, C.-I.: The polar electrojet, *J. Atmos. Terr. Phys.*, 27, 1275–1305, 1965.
- Alexeev, I. I., Belenkaya, E. S., Kalegaev, V. V., Feldstein, Y. I., and Grafe, A.: Magnetic storms and magnetotail currents, *J. Geophys. Res.*, 101, 7737–7747, 1996.
- Alfvén, H.: On the electric field theory of magnetic field and auroras, *Tellus*, 7, 50–64, 1955.
- Allen, J. H. and Kroehl, H. W.: Spatial and temporal distributions of magnetic effects of auroral electrojets as derived from AE indices, *J. Geophys. Res.*, 80, 3667–3677, 1975.
- Allen, J. H., Abston, C. C., and Morris, L. D.: Auroral electrojet magnetic activity indices AE(10) for 1966, Tech. Rep. Report UAG-37, NOAA, Boulder, Colo., 1974.
- Allen, J. H., Abston, C. C., and Morris, L. D.: Auroral electrojet magnetic activity indices AE(10) for 1971, Tech. Rep. Report UAG-39, NOAA, Boulder, Colo., 1975.

- Annals: Annals of the International Geophysical Year (IGY): Ascaplots: half-hourly all-sky camera plots from 114 stations for the period 1957-1958, vol. 20, parts 1 and 2, Pergamon Press, Oxford, International Council of Scientific Unions. Special Committee for the IGY edn., 1962.
- Arykov, A. and Maltsev, Y. P.: Contribution of various sources to the geomagnetic storm field, *Geomagn. Aeron. (Engl. translation)*, 33, 67–74, 1993.
- Arykov, A. A., Belova, E. G., Gvozdevsky, B. B., Maltsev, Y. P., and Safargaleev, V. V.: Geomagnetic storm resulting from enhancement of the high-latitude magnetic flux, *Geomagn. Aeron. (Engl. translation)*, 36, 307–313, 1996.
- Bartels, J. and Fukushima, N.: Ein Q-index für erdmagnetische Aktivität in viertelstündlichen Intervallen, *Abhandlungen Akad. Wiss., Göttingen*, N2, 37p., 1956.
- Bartels, J., Heck, N. H., and Johnston, H. F.: The three-hour range index measuring geomagnetic activity, *Terr. Magn. Atmos. Elect.*, 44, 411–454, 1939.
- Baumjohann, W., Untiedt, J., and Greenwald, R.: Joint two-dimensional observations of ground magnetic and ionospheric electric fields associated with auroral zone currents. 1. Three-dimensional current flows associated with a substorm-intensified eastward electrojet, *J. Geophys. Res.*, 83, 1963–1978, 1980.
- Benkova, N. P.: Diurnal variation of the magnetic activity (in Russian), *Transactions of the Institute of Terrestrial Magnetism*, 3(13), 15–40, 1948.
- Birkeland, K.: The Norwegian Aurorae Polaris Expedition of 1902–1903: On the cause of magnetic storms and the origin of terrestrial magnetism, vol. 1, H. Aschehoug & Co., Christiania, First Section, 1908.
- Birkeland, K.: The Norwegian Aurorae Polaris Expedition of 1902–1903: On the cause of magnetic storms and the origin of terrestrial magnetism, vol. 2, H. Aschehoug & Co., Christiania, Second Section, 1913.
- Bobrov, M.: Types of irregular geomagnetic disturbances and mechanism of the influence of solar corpuscular streams on the outer atmosphere, *Astron. Zhurnal*, 37, 410–424, 1960.
- Boström, R.: A model of the auroral electrojets, *J. Geophys. Res.*, 69, 4983–4994, 1964.
- Bruche, E.: Some new theoretical and experimental results on the aurorae polaris, *Terr. Magn. Atmos. Elect.*, 36, 41–62, 1931.
- Burdo, O. A.: Relation of regular and irregular variations of the geomagnetic field, high latitudes, in: *Transactions of the Arctic and Antarctic Institute*, vol. 223, pp. 21–45, AARI, Leningrad, USSR, 1960.
- Carlheim-Gyllenskiöld, G.: *Exploration internationale des régions polaires, 1882–1883, Observations faites au Cap Thorsden Spitzbergen, par l'expédition suédoise*, T. I, II, Stockholm, 1887.
- Chapman, S.: The electric current systems of magnetic storms, *Terr. Magn. Atmos. Elect.*, 40, 349–370, 1935.
- Chapman, S. and Bartels, J.: *Geomagnetism*, 1, Geomagnetic and related phenomena, Clarendon Press, Oxford, 542p., 1940.
- Davis, T. N. and Sugiura, M.: Auroral electrojet activity index AE and its universal time variations, *J. Geophys. Res.*, 71, 785–801, 1966.
- Feldstein, Y. I.: Geographic distribution of aurorae in the westward sector of Soviet Arctic, *Problems of Arctic*, N4, 45–49, 1958.
- Feldstein, Y. I.: Geographic distribution of aurorae and arcs azimuths, in: *IGY Transactions “Investigations of the aurorae”*, vol. N4, pp. 61–77, Publ. House Academy Sci. USSR, 1960.
- Feldstein, Y. I.: Pattern of the magnetic activity in the high latitudes of the northern hemisphere, in: *Geomagnetism*, vol. N5, Publ. House Academy Sci. USSR, 64p., 1963a.
- Feldstein, Y. I.: The morphology of auroras and geomagnetism, in: *IGY Transactions “Auroras and Airglow”*, vol. N10, pp. 121–125, Publ. House Academy Sci. USSR, 1963b.
- Feldstein, Y. I.: Peculiarities in the auroral distribution and magnetic disturbance distribution in high latitudes caused by the asymmetrical form of the magnetosphere, *Planet. Space Sci.*, 14, 121–130, 1966.
- Feldstein, Y. I.: Magnetic field variations in the polar region during magnetically quiet periods and interplanetary magnetic fields, *Space Sci. Rev.*, 18, 777–861, 1976.
- Feldstein, Y. I. and Galperin, Y. I.: The auroral luminosity structure in the high-latitude upper atmosphere, its dynamics and relationship to the large-scale structure of the Earth's magnetosphere, *Rev. Geophys.*, 23, 217–275, 1985.
- Feldstein, Y. I. and Solomatina, E. K.: Polar auroras in southern hemisphere, *Geomagn. Aeron. (Engl. translation)*, 1, 534–539, 1961.
- Feldstein, Y. I. and Zaitzev, A. N.: Disturbed solar-diurnal variations at high latitudes during the IGY period, *Geomagn. Aeron. (Engl. translation)*, 5, 477–486, 1965a.
- Feldstein, Y. I. and Zaitzev, A. N.: The current system of SD-variations in high latitudes for the winter season during the IGY, *Geomagn. Aeron. (Engl. translation)*, 5, 1123–1128, 1965b.
- Feldstein, Y. I., Sumaruk, P., and Shevnina, N. F.: To the diagnostics of the azimuthal component of the interplanetary magnetic field, *C. R. Acad. Sci. USSR*, 222, 833–836, 1975.
- Feldstein, Y. I., Elphinstone, R. D., Hern, D. J., Murphree, J. S., and Cogger, L. L.: Mapping of the statistical auroral distribution into the magnetosphere, *Can. J. Phys.*, 72, 266–269, 1994.
- Feldstein, Y. I., Popov, V. A., Cumnock, J. A., Prigancova, A., Blomberg, L. G., Kozyra, J. U., Tsurutani, B. T., Gromova, L. I., and Levitin, A. E.: Auroral electrojets and boundaries of plasma domains in the magnetosphere during magnetically disturbed intervals, *Ann. Geophys.*, 24, 2243–2276, 2006.
- Förster, M., Rentz, S., Köhler, W., Liu, H., and Haaland, S. E.: IMF dependence of high-latitude thermospheric wind pattern derived from CHAMP cross-track measurements, *Ann. Geophys.*, 26, 1581–1595, 2008.
- Förster, M., Haaland, S. E., and Doornbos, E.: Thermospheric vorticity at high geomagnetic latitudes from CHAMP data and its IMF dependence, *Ann. Geophys.*, 29, 181–186, 2011.
- Foster, J. C. and Burke, W. J.: SAPS: A new categorization for subauroral electric fields, *EOS*, 83, 393–394, 2002.
- Foster, J. C. and Vo, H. B.: Average characteristics and activity dependence of the subauroral polarization stream, *J. Geophys. Res.*, 107, 1475, doi:10.1029/2002JA009409, 2002.
- Frank, L. A.: Relationship of the plasma sheet, ring current, trapping boundary and plasmapause near the magnetic equator at local midnight, *J. Geophys. Res.*, 76, 2265–2275, 1971.
- Frank, L. A., Van Allen, J. A., and Craven, J. D.: Large diurnal variation of geomagnetically trapped and precipitated electrons observed at low altitudes, *J. Geophys. Res.*, 69, 3155–3167, 1964.
- Friis-Christensen, E. and Wilhjelm, J.: Polar currents for different directions of the interplanetary magnetic field in the Y - Z plane,

- J. Geophys. Res., 80, 1248–1260, 1975. 2330
- Friis-Christensen, E., Laasen, K., Wilhjelm, J., Wilcox, J. M., Gonzalez, W., and Colburn, D. S.: Critical Component of the Interplanetary Magnetic Field Responsible for Large Geomagnetic Effects in the Polar Cap, *J. Geophys. Res.*, 77, 3371–3376, 1972. 2334
- Fukushima, N.: Polar magnetic storms and geomagnetic bays, vol. 8, Part V of *Series II*, pp. 293–412, Geophysical Institute, Faculty of Science, Tokyo University, Tokyo, Japan, 1953. 2337
- Fukushima, N. and Oguti, T.: Polar magnetic storms and geomagnetic bays, Appendix 1, A theory of SD field, in: *Rep. Ionosph. Res. in Japan*, vol. 7, No. 4, pp. 137–145, Geophysical Institute, Faculty of Science, Tokyo University, Tokyo, Japan, 1953. 2340
- Galperin, Y. and Feldstein, Y. I.: Auroral luminosity and its relationship to magnetospheric plasma domains, pp. 207–222, Cambridge University Press, ed. by C.-I. Meng, M. J. Rycroft, and A. Frank, 1991. 2345
- Galperin, Y. I.: Polarization Jet: characteristics and a model, *Ann. Geophys.*, 20, 391–404, 2002. 2347
- Galperin, Y. I. and Feldstein, Y. I.: Mapping of the precipitation regions to the plasma sheet, *J. Geomag. Geoelectr.*, 48, 857–875, 1996. 2349
- Galperin, Y. I., Ponomarev, V. N., and Zosimova, A. G.: Plasma convection in the polar ionosphere, *Ann. Geophys.*, 30, 1–7, 1974. 2353
- Gonzalez, W. D., Joselyn, J. A., Kamide, Y., Kroehl, H. W., Rostoker, G., Tsurutani, B. T., and Vasyliunas, V. M.: What is a geomagnetic storm?, *J. Geophys. Res.*, 99, 5771–5792, 1994. 2356
- Grafe, A., Bessalov, P. A., Trakhtengerts, V. Y., and Demekhova, A. G.: Afternoon mid-latitude current system and low-latitude geomagnetic field asymmetry during geomagnetic storm, *Ann. Geophys.*, 15, 1537–1547, 1997. 2360
- Gustafsson, G.: A revised corrected geomagnetic coordinate system, *Arkiv for Geofysik*, 5, 773–, 1970. 2362
- Harang, L.: The mean field of disturbance of polar geomagnetic storms, *Terr. Magn. Atmos. Elect.*, 51, 353–380, 1946. 2364
- Harang, L.: *The Aurorae*, vol. 1, Chapman & Hall, Ltd., London, The International Astrophysical Series edn., 163p., 1951. 2366
- Heppner, J.: The Harang discontinuity in auroral belt ionospheric current, *Geofysiske Publikasjoner*, 29, 105–120, 1972. 2368
- Hope, E. R.: Low-latitude and high-latitude geomagnetic agitation, *J. Geophys. Res.*, 66, 747–776, 1961. 2370
- Hulburt, E. O.: On the diurnal variation of the aurora polaris, *Terr. Magn. Atmos. Elect.*, 36, 23–40, 1931. 2372
- Hultqvist, B.: The geomagnetic field lines in higher approximations, *Arkiv Geofysik*, 3, 63–77, 1958. 2374
- Isaev, S. I.: About diurnal periodicity of auroras inside the zone of maximal frequency, *Problems of the Arctic*, 9, 41–45, 1940. 2376
- Isaev, S. I. and Pushkov, N. V.: *The Aurorae*, Publ. House Academy Sci. USSR, 112p., 1958. 2378
- Kamide, Y. and Akasofu, S.-I.: Latitudinal cross section of the auroral electrojet and its relation to the interplanetary magnetic field polarity, *J. Geophys. Res.*, 79, 3755–3771, 1974. 2381
- Kamide, Y., Ahn, B.-H., Akasofu, S.-I., Baumjohann, W., Friis-Christensen, E., Kroehl, H. W., Maurer, H., Richmond, A. D., Rostoker, G., Spiro, R. W., Walker, J. R., and Zaitzev, A. N.: Global distribution of ionospheric and field-aligned currents during substorms as determined from six meridian chains of magnetometers: initial results, *J. Geophys. Res.*, 87, 8228–8240, 1982. 2387
- Kamide, Y., Baumjohann, W., Daglis, I. A., Gonzalez, W. D., Grande, M., Joselyn, J. A., McPherron, R. L., Phillips, J. L., Reeves, E. G. D., Rostoker, G., Sharma, A. S., Singer, H. J., Tsurutani, B. T., and Vasyliunas, V. M.: Current understanding of magnetic storms: Storm-substorm relationships, *J. Geophys. Res.*, 103, 17,705–17,728, 1998. 2390
- Killeen, T. L. and Roble, R. G.: *Thermosphere Dynamics: Contributions from the First 5 Years of the Dynamics Explorer Program*, *Rev. Geophys.*, 26, 329–367, 1988. 2393
- Korotik, A. B. and Pudovkin, M. I.: About possible mechanism of magnetic disturbances origin, in: *Transactions “Spectral, electro-photometrical and radiolocation investigations of auroras”*, vol. N6, pp. 37–42, Publ. House Academy Sci. USSR, 1961. 2396
- Kotikov, A. L., Bolotynskaya, B. D., Gizler, V. A., Troshichev, O. A., Pashin, A. B., and Tagirov, V. R.: Structure of auroral zone phenomena from the data of meridional chains of stations: magnetic disturbances in the night-time auroral zone and auroras, *J. Atmos. Terr. Phys.*, 53, 265–277, 1991. 2399
- Lassen, K.: Existence of an inner auroral zone, *Nature*, 184, 1375–1377, 1959a. 2402
- Lassen, K.: Local aurorae in the morning hours at Godhavn, in: *Meddelelser*, vol. N 24, Det Danske Meteor. Inst., Charlottenlund, 1959b. 2405
- Lassen, K.: Day-time aurorae observed at Godhavn 1954–1956, in: *Meddelelser*, vol. Medd. N 15, Det Danske Meteor. Inst., Charlottenlund, 1961. 2408
- Lassen, K.: Geographical distribution and temporal variations of polar aurorae, in: *Meddelelser*, vol. 16, Det Danske Meteor. Inst. Meddelelser, Charlottenlund, 1963. 2411
- Liemohn, M. W., Kozyra, J. U., Thomsen, M. F., Roeder, J. L., Lu, G., Borovsky, J. E., and Cayton, T. E.: Dominant role of the asymmetric ring current in producing the stormtime Dst\*, *J. Geophys. Res.*, 106, 10,883–10,904, 2001. 2414
- Lühr, H., Rentz, S., Ritter, P., Liu, H., and Häusler, K.: Average thermospheric wind pattern over the polar regions, as observed by CHAMP, *Ann. Geophys.*, 25, 1093–1101, 2007. 2417
- Lyatsky, W., Maltsev, Y. P., and Leontyev, S. V.: Three-dimensional current system in the different phases of a substorm, *Planet. Space Sci.*, 22, 1231–1247, 1974. 2420
- Maltsev, Y. P.: Points of controversy in the study of magnetic storms, *Space Sci. Rev.*, 110, 227–267, 2004. 2423
- Maltsev, Y. P. and Ostapenko, A. A.: Field-aligned currents in the ionosphere and magnetosphere, in: *Proceedings of the International Symposium in memory of Yuri Galperin on ‘Auroral Phenomena and Solar-Terrestrial Relations’*, edited by Zelenyi, L. M., Geller, M. A., and Allen, J. H., pp. 147–151, IKI, Moscow, 4–7 February 2003, 2004. 2426
- Malville, J. M.: Antarctic auroral observations, Ellsworth Station, 1957, *J. Geophys. Res.*, 64, 1389–1393, 1959. 2429
- Mansurov, S. M.: New evidence of the relationship between magnetic field in space and on the Earth, *Geomagn. Aeron. (Engl. translation)*, 9, 768–773, 1969. 2432
- Mansurov, S. M. and Mishin, V. M.: Diurnal behaviour of magnetic activity in the polar region, in: *Transactions “Earths electromagnetic field disturbances”*, pp. 45–52, USSR Academy of Science Publishing House, 1960. 2435
- Marghitu, O., Karlsson, T., Klecker, B., Haerendel, G., and McFadden, J.: Auroral arcs and oval electrodynamic in the Harang region, *J. Geophys. Res.*, 114, A03214, doi:10.29/2008JA013630, 2009. 2438

- 2389 2009. 2448
- 2390 Mayaud, P.: Activite magnetique dans les regions polaires, Rap-2449  
ports scientifiques des expeditions polaires francaises, Annales2450  
2391 de géophysique, 12, 84–101, 1956. 2451
- 2392 Mayaud, P. N.: Calcul preliminaire d'indices Km, Kn, Ks, ou Am2452  
2393 An et As, mesures de l'activite magnetique a l'echelle et dans les2453  
2394 hemispheres Nord et Sud, Annales de géophysique, 23, 585–617,2454  
2395 1967. 2455
- 2396 Mayaud, P. N.: The aa indices: a 100 year series characterizing the2456  
2397 magnetic activity, *J. Geophys. Res.*, 77, 6870–6874, 1972. 2457
- 2398 Meek, J. H.: The location and shape of the auroral zone, *J. Atmos.*2458  
2400 *Terr. Phys.*, 6, 313–321, 1955. 2459
- 2401 Nagata, T. and Fukushima, N.: Constitution of polar magnetic2460  
2402 storms, *Rep. Ionos. Res. Japan*, 6, 85–96, 1952. 2461
- 2403 Nagata, T., Fukushima, N., and Sugiura, M.: Electro-dynamical be-2462  
2404 haviour of the ionosphere region viewed from geomagnetic vari-2463  
2405 ations, *J. Geomag. Geoelectr.*, 2, 35–44, 1950. 2464
- 2406 Neumayer, G. and Börgen, C.: Die Internationale Polarforschung2465  
2407 1882–1883, Die Beobachtungs-Ergebnisse der Deutschen Sta-2466  
2408 tionen, vol. 1, Kingua Fjord, Asher, Berlin, 1886. 2467
- 2409 Nikolsky, A. P.: Dual laws of the course of magnetic disturbances2468  
2410 and the nature of mean regular variations, *Terr. Magn. Atmos.*2469  
2411 *Elect.*, 52, 147–173, 1947. 2470
- 2412 Nikolsky, A. P.: Magnetic disturbances in the Arctic, vol. 36, AARI2471  
2413 Leningrad, USSR, 135p., 1951. 2472
- 2414 Nikolsky, A. P.: On the second zone of magnetic disturbances inten-2473  
2415 sity increased in near-polar region, in: Transactions of the Arc-2474  
2416 tic and Antarctic Institute, vol. 83, pp. 5–83, AARI, Leningrad,2475  
2417 USSR, 1956. 2476
- 2418 Nikolsky, A. P.: On planetary distribution of magneto-ionospheric2477  
2419 disturbances, in: Transactions of the Arctic and Antarctic Insti-2478  
2420 tute, vol. 223, pp. 3–20, AARI, Leningrad, USSR, 1960a. 2479
- 2421 Nikolsky, A. P.: On the issue of geographical distribution of auroras2480  
2422 in Arctic, in: Transactions “Investigation of aurorae”, vol. 4, pp.2481  
2423 14–19, USSR Academy of Science Publishing House, Moscow,2482  
2424 1960b. 2483
- 2425 Nishida, A.: Formation of the plasmopause, or magnetospheric2484  
2426 plasma knee, by the combined action of magnetospheric con-2485  
2427 vection and plasma escape from the tail, *J. Geophys. Res.*, 71,2486  
2428 5669–5679, 1966. 2487
- 2429 O'Brien, B. J.: A large diurnal variation of the geomagnetically2488  
2430 trapped radiation, *J. Geophys. Res.*, 68, 989–997, 1963. 2489
- 2431 Paschmann, G., Haaland, S., and Treumann, R., eds.: *Auro-*2490  
2432 *ral Plasma Physics*, vol. 15 of *Space Sciences Series of ISSI*2491  
2433 *(SSSI)*, Kluwer Academic Publishers, Dordrecht, Boston, Lon-2492  
2434 don, reprinted from *Space Science Reviews* Volume 103, No.2493  
2435 1–4, 2002. 2494
- 2436 Popov, V. and Feldstein, Y. I.: About a new interpretation of “Ha-2495  
2437 rang discontinuity”, *Geomagn. Aeron. (Engl. translation)*, 36,2496  
2438 43–51, 1996. 2497
- 2439 Popov, V. A., Papitashvili, V. O., and Watermann, J. F.: Modeling2498  
2440 of equivalent ionospheric currents from meridian magnetometer2499  
2441 chain data, *Earth, Planets and Space*, 53, 129–137, 2001. 2500
- 2442 Pudovkin, M. I.: Origins of bay disturbances, in: *Series Geophys.*2501  
2443 vol. No. 3, pp. 484–489, *Izvest. Acad. Nauk*, 1960. 2502
- 2444 Pudovkin, M. I.: Magnetic bay disturbance (in Russian), in: Trans-2503  
2445 actions “Investigations on geophysical phenomena of the elec-2504  
2446 tromagnetic complex at high latitudes”, pp. 3–22, Publ. House2505  
2447 Nauka, USSR, 1964. 2506
- Pudovkin, M. I.: Diurnal variation of the ionospheric drift velocity  
in the auroral zone and the SD variations (in Russian), in: Trans-  
actions “Investigations of auroras, geomagnetic disturbances and  
the ionosphere at high latitudes”, pp. 3–10, Publ. House Nauka,  
USSR, 1965a.
- Pudovkin, M. I.: Some remarks on the dynamo theory of geomag-  
netic disturbances (in Russian), in: Transactions “High-latitude  
Investigations in the field of geomagnetism and aeronomy”, pp.  
19–26, Publ. House Nauka, USSR, 1965b.
- Pudovkin, M. I.: Morphology and nature of polar magnetic storms  
(in Russian), Ph.D. thesis, Leningrad University, dSc Disserta-  
tion, 1968.
- Pudovkin, M. I. and Evlashin, L. S.: Spatial relationship of auroras  
with electric currents in the ionosphere (in Russian), *Geomagn.  
Aeron. (Engl. translation)*, 2, 669–673, 1962.
- Pudovkin, M. I. and Korotin, A. B.: Magnetic bay disturbances and  
their relation to ionospheric drifts (in Russian), *Geomagn. Aeron.*  
(Engl. translation), 1, 408–412, 1961.
- Pushkov, N. V., Brunkovskaya, N. S., and Abramova, N. V.: Com-  
parison of magnetic and auroral activities according to observa-  
tions at Tikhaya Bay in 1932–1933 (in Russian), *Transactions*  
“Earth magnetism and Electricity”, 4, 71–75, 1937.
- Richmond, A. D., Lathuillère, C., and Vennerstroem, S.: Winds  
in the high-latitude lower thermosphere: Dependence on the in-  
terplanetary magnetic field, *J. Geophys. Res.*, 108, 1066, doi:  
10.1029/2002JA009493, 2003.
- Sandholt, P. E., Farrugia, C. J., and Denig, W. F.: Detailed day-  
side auroral morphology as a function of local time for south-  
ern IMF orientation: implications for solar wind-magnetosphere  
coupling, *Ann. Geophys.*, 22, 3537–3560, 2004.
- Stagg, J. M.: The diurnal variation of magnetic disturbances in high  
latitudes, *Proc. R. Soc., A*, 152, 277–298, 1935.
- Starkov, G. V. and Feldstein, Y. I.: Instantaneous distribution of au-  
roras and polar geomagnetic disturbances, in: Transactions “Au-  
roras”, vol. N19, pp. 32–41, USSR Academy of Science Publish-  
ing House, 1970.
- Steward, B.: *Terrestrial magnetism*, vol. 16, pp. 159–184, Gordon  
and Breach, New York, 9th ed., 1882.
- Stoffregen, W.: Instructions for scaling auroral ascaplots and au-  
roral indices, in: *Medd., Repot N5, Uppsala Ionosfarobservato-  
rium*, 1959.
- Størmer, C.: Corpuscular theory of the aurorae borealis, *Terr. Magn.*  
*Atmos. Elect.*, 22, 23–34, 1917a.
- Størmer, C.: Corpuscular theory of the aurorae borealis. (con-  
cluded), *Terr. Magn. Atmos. Elect.*, 22, 97–112, 1917b.
- Størmer, C.: *The Polar Aurora*, Clarendon Press, 402p., 1955.
- Sugiura, M.: Hourly values of equatorial Dst for the IGY, in:  
*Annals of the International Geophysical Year (I.G.Y.)*, edited  
by of Scientific Unions. Special Committee for the IGY, I. C.,  
vol. 35, pp. 9–???, Pergamon Press, Oxford, 1964.
- Sumaruk, P. V. and Feldstein, Y. I.: Sector structure of the interplan-  
etary magnetic field and the magnetic variations in the near-polar  
region (in Russian), *Kosm. Issled.*, 11, 155–160, 1973.
- Svalgaard, L.: Sector structure of the interplanetary magnetic field  
and daily variation of the geomagnetic field at high latitudes, in:  
*Geophys. Papers*, R-6, Danish Meteorol. Inst., 1968.
- Tikhonov, A. N. and Arsenin, V. I.: Solutions of ill-posed problems,  
*Scripta series in mathematics*, Halsted Press, New York, 258p.,  
1977.

- 2507 Tromholt, S.: Sur les periodes de laurore boreale, Dan. Meteor. Inst.  
2508 Copenhagen, 1882.
- 2509 Troshichev, O. A., Andrezen, V. G., Vennerstrom, V. G., and Friis-  
2510 Christensen, E.: Magnetic activity in the polar cap A new index,  
2511 Planet. Space Sci., 36, 1095–1102, 1988.
- 2512 Troshichev, O. A., Janzhura, A. S., and Stauning, P.: Unified PCN  
2513 and PCS indices: method of calculation, physical sense and de-  
2514 pendence on the IMF azimuthal and northward components, J.  
2515 Geophys. Res., 111, A05208, doi:10.1029/2005JA011402, 2006.
- 2516 Untiedt, J. and Baumjohann, W.: Studies of polar current systems  
2517 using the IMS Scandinavian magnetometer array, Space Sci.  
2518 Rev., 63, 245–390, 1993.
- 2519 Vasyliunas, V. M.: Low energy particle fluxes in the geomagnetic  
2520 tail, pp. 25–47, Gordon and Breach, New York, 1970.
- 2521 Vegard, L.: On the properties of the rays producing aurorae borealis,  
2522 Philos. Mag., 23, 211–237, 1912.
- 2523 Whitham, K. and Loomer, E. J.: A comparison of magnetic dis-  
2524 turbance at Resolute Bay and Baker Lake, Tellus, 8, 276–278,  
2525 1956.
- 2526 Whitham, K., Loomer, E. J., and Niblett, E. R.: The latitudinal dis-  
2527 tribution of magnetic activity in Canada, J. Geophys. Res., 65,  
2528 3961–3974, 1960.
- 2529 Winningham, J. D., Yasuhara, F., Akasofu, S.-I., and Heikkila,  
2530 W. J.: The latitudinal morphology of 10-eV to 10-keV electron  
2531 fluxes during magnetically quiet and disturbed times in the 2100-  
2532 0300 MLT sector, J. Geophys. Res., 80, 3148–3171, 1975.
- 2533 Zhigalova, N. N. and Ol, A. I.: High-latitude bay disturbances of the  
2534 geomagnetic field (in Russian), Problems of Arctic and Antarc-  
2535 tic, 15, 69–73, 1964.
- 2536 Zou, S., Lyons, L. R., Wang, C.-P., Boudouridis, A., Ruohoniemi,  
2537 J. M., Anderson, P. C., Dyson, P. L., and Devlin, J. C.: On  
2538 the coupling between the Harang reversal evolution and sub-  
2539 storm dynamics: A synthesis of SuperDARN, DMSP, and IM-  
2540 AGE observations, J. Geophys. Res., 114, A01205, doi:10.1029/  
2541 2008JA013449, 2009.